Experimental Dermatology ADF

Self-organizing hair peg-like structures from dissociated skin progenitor cells: New insights for human hair follicle organoid engineering and Turing patterning in an asymmetric morphogenetic field

Journal:	*Experimental Dermatology*
Manuscript ID	EXD-18-0381.R1
Manuscript Type:	Regular Article
Date Submitted by the Author:	02-Jan-2019
Keywords:	Skin reconstitution, tissue engineering, hair follicle, periodic pattern formation, organogenesis

Complete List of Authors:
Weber, Erin; Keck School of Medicine of the University of Southern California, Pathology; Keck Hospital of USC, Plastic and Reconstructive Surgery
Woolley, Thomas; Cardiff University, Mathematics
Yeh, Chao-Yuan; University of Southern California, Pathology
OU, KUANG-LING; Keck School of Medicine of the University of Southern California, Pathology; Tri-Service General Hospital, Plastic Surgery
Maini, Philip; University of Oxford, Wolfson Centre for Mathematical Biology
Chuong, Cheng Ming; University of Southern California ,

Note: The following files were submitted by the author for peer review, but cannot be converted to PDF. You must view these files (e.g. movies) online.

Movie S1A.mp4
Movie S1B.mp4
Movie S1C.mp4
Movie S2A.mp4
Movie S2B.mp4
Movie S3A.mp4
Movie S3B.mp4
Movie S4.mp4
Movie S5A.mp4
Movie S5B.mp4
Movie S6.mp4

Self-organizing hair peg-like structures from dissociated skin progenitor cells: New insights for human hair follicle organoid engineering and Turing patterning in an asymmetric morphogenetic field

Running title: Self-organization of hair peg-like structures

Erin L. Weber, M.D., Ph.D.[1,2]

Thomas E. Woolley, Ph.D.[3]

Chao-Yuan Yeh, M.D.[1]

Kuang-Ling Ou, M.D.[1,4,5]

Philip K. Maini, Ph.D.[6]

Cheng-Ming Chuong, M.D., Ph.D.[1,7,*]

[1] Department of Pathology, Keck School of Medicine of the University of Southern California, Los Angeles, CA

[2] Division of Plastic and Reconstructive Surgery, Keck School of Medicine of the University of Southern California, Los Angeles, CA

[3] Cardiff School of Mathematics, Cardiff University, Senghennydd Road, Cardiff, CF24 4AG, UK.

[4] Ostrow School of Dentistry of the University of Southern California, Los Angeles, CA

[5] Division of Plastic and Reconstructive Surgery, Department of Surgery, Tri-Service General Hospital, National Defense Medical Center, Taipei, Taiwan

[6] Wolfson Centre for Mathematical Biology, Mathematical Institute, Oxford, OX2 6GG, UK.

[7] Integrative Stem Cell Center, China Medical University, Taichung, Taiwan

Corresponding author: Cheng-Ming Chuong, M.D., Ph.D.
Keck School of Medicine of the University of Southern California
2011 Zonal Ave, HMR 313B
Los Angeles, CA 90089
cmchuong@usc.edu

Word count: 5347

Abstract

Human skin progenitor cells will form new hair follicles, although at a low efficiency, when injected into nude mouse skin. To better study and improve upon this regenerative process, we developed an *in vitro* system to analyze the morphogenetic cell behavior in detail and modulate physical-chemical parameters to more effectively generate hair primordia. In this three-dimensional culture, dissociated human neonatal foreskin keratinocytes self-assembled into a planar epidermal layer while fetal scalp dermal cells coalesced into stripes, then large clusters, and finally small clusters resembling dermal condensations. At sites of dermal clustering, subjacent epidermal cells protruded to form hair peg-like structures, molecularly resembling hair pegs within the sequence of follicular development. The hair peg-like structures emerged in a coordinated, formative wave, moving from periphery to center, suggesting that the droplet culture constitutes a microcosm with an asymmetric morphogenetic field. *In vivo*, hair follicle populations also form in a progressive wave, implying the summation of local periodic patterning events with an asymmetric global influence. To further understand this global patterning process, we developed a mathematical simulation using Turing activator-inhibitor principles in an asymmetric morphogenetic field. Together, our culture system provides a suitable platform to 1) analyze the self-assembly behavior of hair progenitor cells into periodically arranged hair primordia, and 2) identify parameters that impact the formation of hair primordia in an asymmetric morphogenetic field. This understanding will enhance our future ability to successfully engineer human hair follicle organoids.

Key words

Skin reconstitution, tissue engineering, hair follicle, periodic pattern formation, organogenesis

Introduction

The basic tenet of plastic surgery is the restoration of form and function. However, replacing skin and functional appendages remains challenging. The hair follicle is a mini-organ, which, in association with the attached sebaceous gland, plays a crucial role in skin moisture, thermal regulation, protective sensation, and aesthetic appearance. For burn patients, the loss of pilosebaceous units leads to dry, brittle skin which is more susceptible to injury. While transplantation is currently the best option for hair follicle replacement, the process requires a large number of donor follicles, which burn patients typically lack, and targets only the scalp. The ability to tissue engineer an unlimited source of pilosebaceous units for transplantation, either singly or appropriately patterned within bioengineered skin, would provide a much-needed solution for many patients.

Multiple different approaches have attempted to produce reconstituted skin with hair in mouse and human.[1] In the mouse, we demonstrated that dissociated epidermal and dermal cells from newborn mouse skin self-assemble *in vitro* into multilayered skin organoids containing placodes and dermal condensates, the two stem cell populations necessary for hair follicle development.[2, 3] When grafted onto a full thickness dermal wound on a nude mouse, the cultured organoids formed mature, cycling hair follicles within a planar skin configuration. Transcriptomic analysis of the murine skin organoids has identified factors that can rescue the hair forming ability of adult mouse cells.[4] However, similar success with human cells has been more difficult. Adult human scalp cells will produce new follicles in *in vivo* mouse models, albeit at low rates.[5, 6] The use of fetal, rather than adult, scalp enhances the efficiency of human hair follicle regeneration but a persistent lag time of three months to follicle formation indicates that more must be understood about follicular morphogenesis.[7, 8] Despite several different approaches, efficient, large-scale, therapeutic tissue engineering and transplantation of reconstituted human skin with pilosebaceous units remains a challenge to the field.

There are two different strategies to produce hair follicles from dissociated cells. One is to use 3D printed tissue scaffolds and place cells at key positions for further morphogenesis;[9] the other is to rely on the self-organizing ability of skin progenitor cells.[4] Different progenitor cell states can be utilized for the self-organizing strategy, such as induced pluripotent cells (iPS).[10] On some occasions, cells need "help" to interact with other cells or require particular molecular signals to move forward to the next stage. Currently, in the emerging field of synthetic biology, methods are under development to provide cells with "help" in topological arrangement [11, 12] or molecular signaling at the right time and place.[13]

But, to effectively adopt the synthetic biology approach, we must learn more about organoid cultures made of cells from different ages, locations, or species, so we can apply key molecules to restore hair forming ability.[4] To this end, we sought to develop a three-dimensional, culture system in which different types of skin progenitors, such as epidermal- or dermal-like somatic cells, embryonic stem cells, or iPS cells, can be guided to form ectodermal organs in a planar configuration (Fig. S1).[14] We hope that this culture model may serve as a platform to identify the critical factors needed, step by step, for the development of individual ectodermal organs. Here, we present our progress toward the formation of human hair follicle organoids. Within this *in vitro* model, we observed two distinct and novel phenomena. First, hair peg-like structures emerged after only four days in culture and possessed molecular and cellular characteristics similar to authentic human hair pegs. Second, the formative process of periodic patterning was quite apparent: dissociated dermal cells assembled into stripes, clusters, then distinct dermal condensations, followed by epidermal "stalks" with dermal papilla-like "caps". The process reproducibly began at the droplet boundary and emanated as a circumferential wave toward the center of the culture.

In vivo, periodic hair and feather placodes form in a progressive wave, propagating in different directions depending on body site (e.g., scalp and trunk). This implies that the process is a combination of local periodic patterning events and an asymmetric global influence that make the morphogenetic field asymmetric. The local periodic patterning event may involve chemical and mechanical feedback between cells and their environment.[15, 16] Several models have been proposed, ranging from chemical-based reaction-diffusion models to ones where the "reactants" are cells themselves to mechanochemical models which couple cell interactions with chemical signals.[17-19] The self-organizing patterns observed experimentally in our culture system resemble patterns most simply illustrated by the Turing activator-inhibitor model.[20, 21] The global behavior of the system can be described by the occurrence of a Turing instability on an asymmetric morphogenetic field. Such asymmetry is speculated to be caused by mechanical or chemical forces or uneven cell proliferation or death.[22, 23]

The droplet culture system described here provides a unique opportunity to study both periodic patterning and global events in human hair follicle formation. The formation of hair peg-like structures occurs more rapidly than other current methods and, yet, is slow enough to permit the analysis and optimization of the sequence of cellular events. Mathematical modeling of the formation wave in the hair peg population allows us to analyze the self-assembly process and predict conditions that may enhance organoid formation. Translationally, this culture system provides proof of concept that structures resembling human hair follicle precursors can be engineered *in vitro* in a time-efficient manner and serves

as a platform to identify the optimal conditions with which to efficiently engineer human hair follicles for transplantation.

Methods

In vitro hair follicle reconstitution assay

Epidermal and dermal cells were enzymatically and mechanically separated from neonatal foreskin and second trimester fetal scalp (estimated gestational age (EGA) 17-19 weeks), respectively. $2x10^6$ cultured neonatal foreskin keratinocytes and $3x10^6$ fresh fetal scalp dermal cells were resuspended in 140 ul of F12:DMEM (1:1) medium with 5% FBS and P/S/A and plated as a droplet on a 6-well cell culture insert. The droplets were incubated at 37°C and 5% CO_2 for 4-7 days. Growth factors were added daily. See supplemental methods for details.

Patch assay

$2x10^6$ neonatal foreskin keratinocytes and $3x10^6$ fetal scalp dermal cells were injected subcutaneously into the deep dermis of 6-12 week old hairless nude mice. Subcutaneous nodules with formed hair follicles were harvested 8 weeks later.

Immunostaining, lentiviral vectors, and live cell imaging

See supplemental methods.

Mathematical modeling

A reaction-diffusion model was developed to simulate the interaction of two, as of yet, experimentally unidentified, different morphogen populations. Details, equations, and parameter definitions are included in supplemental methods.

Results

Human fetal scalp dermal cells induce the self-organization of hair peg-like structures in droplet culture

Dissociated neonatal human foreskin keratinocytes and 17-19 week EGA human fetal scalp dermal cells were mixed and co-cultured in three-dimensional droplets (Fig. 1A). Within 24 hours, the epidermal and dermal cells segregated into two layers, with epidermal cells adhering to the cell culture insert membrane at the base of the droplet and dermal cells overlying the keratinocytes in a more superficial layer (Fig. 1B). Around 48 hours, dermal cells began to organize, forming a trabecular mesh pattern, which then evolved into punctate cell clusters. By 72 hours, keratinocytes abutting the dermal clusters rearranged into a concentric pattern and, within 96 hours, keratinocyte "stalks" protruded, against gravity, into the droplet space, in association with a dermal cell "cap", (Fig. 1B, Movie S1A-C). In comparison with 17-week EGA fetal scalp sections, the newly formed structures resemble early hair pegs, a stage in follicle development in which the invaginating keratinocytes protrude downward into the dermal plane, guided by the dermal papilla (Fig. 1C). Of note, while there was a clear and early segregation of epidermal and dermal cells, we frequently encountered scattered, large, intensely keratin-positive cells interspersed within the dermal layer, which exhibited characteristics consistent with terminally differentiated, anucleated keratinocytes. These "cells" do not appear to participate in the morphological events.

Dermal fibroblasts are known to self-aggregate in non-adherent culture. To demonstrate that the hair peg-like structures were not an artifact of the culture system or simply a result of dermal fibroblast self-aggregation, human fetal scalp dermal cells, in the absence of foreskin keratinocytes, were cultured under identical conditions. Fetal scalp dermal cells also formed a trabecular pattern but did not form any three-dimensional structures (Fig. 1D). Similarly, adult dermal cells, from hair-bearing adult scalp, were cultured with neonatal foreskin keratinocytes. Adult scalp dermal cells formed thick, dense sheets. Neither combination produced hair peg-like structures.

Hair peg-like structures in vitro displayed cytoarchitecture and molecular markers similar to those observed in vivo.

Under defined conditions, epidermal and dermal cells rapidly self-assembled and transitioned through stages reminiscent of follicular development to form hair peg-like structures but failed to progress further *in vitro*. To verify that the human neonatal foreskin keratinocytes and human fetal scalp dermal cells possessed full regenerative potential, the same ratio of epidermal and dermal cells was injected

subcutaneously into nude mice in a traditional patch assay.[2] Eight weeks later, complete hair follicles, including hair shafts, were clearly visible in the subcutaneous tissue encircling a central keratinized mass (Fig. 1E). Immunostaining with human-specific antibodies confirmed that cells of the epidermal outer root sheaths and dermal papillae were of human origin (Fig. 1E).

Akin to hair pegs in developing fetal skin, the reconstituted hair peg-like structures were keratin-14 positive and keratin-10 negative (Fig. 2A). Keratin-10 and involucrin, markers of suprabasal cells, were expressed in all cells of the epidermal sheet except the basal layer, consistent with normal patterns of epidermal stratification (Fig. 2A). While epidermal cells originally stratified with basement membrane facing the insert, the polarity of stratification was altered once epidermal downgrowth began, with epidermal "stalks" and associated dermal "caps" projecting upwards into the culture through more differentiated layers of epidermis. We suspect this is due to physical limitations of the droplet culture system. Keratinocytes of the epidermal stalk expressed K17, K18, and E-cadherin, all known to be expressed in the inner or outer root sheath layers of mature follicles, though at the hair peg stage, distinct epidermal sheath layers have not yet formed and less is known about the expected locations for expression of these proteins (Fig. 2A). Some of the larger hair peg-like structures displayed longer, curving epidermal stalks, which when viewed at the right angle, appeared to possess a central keratin-positive core surrounded by concentrically-oriented epidermal cells, possibly indicating progression in development towards the bulbous peg stage (Fig. 2A). These advanced hair peg-like structures occurred infrequently, however, making further characterization difficult.

p63, a marker of epidermal stem cells, was initially present in all keratinocytes at 24 hrs. As is seen in normal hair follicle development, p63 expression became limited to the basal layer following epidermal stratification and p63-positive cells were reproducibly noted at the leading edge of the epidermal stalk, adjacent to the dermal cap (Fig. 2B). PCNA immunostaining demonstrated active cell division in both the epidermal basal layer and the leading edge of the stalk, while the remaining epidermal cells within the stalk were quiescent (Fig. 2B). The presence of focal, replicating epidermal progenitor cells at the leading edge of the stalk suggests that localized proliferation may contribute to downgrowth and we hypothesize that these proliferating cells may be putative hair matrix cells. However, we cannot rule out the possible contribution of cell migration from the adjacent stratified epidermis in hair peg formation and the mechanism by which epidermal downgrowth occurs is not yet known.

Consistent with a dermal lineage, dermal cap cells synthesized collagens I and III (Fig. 2C). Basement membrane proteins, collagen IV and laminin, typically located at the interface between epidermal and mesenchymal cells within the hair follicle, were present at the junction of epidermal stalk

and the dermal cap (Fig. 2C, Movie S2A). Furthermore, the dermal cap cells associated with the hair peg-like structures displayed markers also present in the dermal condensate and dermal papilla. The dermal cap was composed of a heterogeneous mixture of dermal cells with a central compartmentalized area positive for alpha-smooth muscle actin (α-SMA, Fig. 2C, Movie S2B). While alkaline phosphatase is a classic marker of the murine dermal papilla and is expressed in the dermal papillae of 17-week human fetal scalp, there is limited and conflicting data regarding the expression of alkaline phosphatase versus α-SMA in human dermal papilla cells in culture. Some publications show persistent alkaline phosphatase expression in cultured human dermal papilla cells but others demonstrate rapid loss of alkaline phosphatase expression and upregulation of α-SMA expression.[24-29] In reality, the expression of dermal papilla marker genes is easily influenced by culture conditions. In our system, α-SMA expression was present while alkaline phosphatase expression was not. Versican, another commonly used marker for the dermal condensate and papilla, was strongly expressed in the dermal cap (Fig. 2B, C). While these dermal caps represent the developmental progression of dermal stripes to clusters to condensations and dermal papillae-like aggregates, which can functionally induce hair-peg like structures, we believe they are incomplete or immature dermal papillae because they express some, but not all, dermal papilla molecular markers and induce the formation of hair peg-like structures instead of complete hair follicles.

The formation of hair peg-like structures in vitro mimics the sequential stages of development in vivo

Foreskin keratinocytes and fetal scalp dermal cells progressed through stages similar to native hair follicle development.[30] Between 48 and 72 hours in culture, epidermal cells underlying focal dermal cell collections formed a concentric pattern, distinct from the cobblestone pattern of the surrounding epidermal sheet (Fig. 2D, Movie S3A,B).[31] β-catenin, known to be expressed in the epidermal placode and required for hair follicle morphogenesis, was focally enriched in epidermal cells abutting the clustered dermal cells, but absent from the adjacent epidermis at the time of epidermal downgrowth (Fig. 2E).[32-34] Cells within the dermal clusters expressed CD34, a marker of the human dermal condensate and early dermal papilla (Fig. 2E).[35] The formation of hair germ-like structures and, then, hair peg-like structures ensued between 72-96 hours in culture.

Live cell confocal imaging of the droplet culture was developed to visualize the cell-cell interactions and collective cell movements during hair peg formation. Visual discrimination between epidermal and dermal cells was achieved using epidermal-specific promoters. Lentiviral transduction to express lineage-specific fluorescent markers did not perturb hair peg development *in vitro* (Fig. S2). A view from the top of a two-color, live cell culture droplet demonstrated distinct spherical dermal caps is shown

in the Supplement Material (Fig. S2**,** Movie S4). Nuclei of cells at the periphery of the dermal cap exhibited a curved morphology and cells near the center of the dermal cap displayed increased local cell motion while cells at the periphery were more stationary, suggesting a heterogeneity of dermal cell function. In contrast, cells within the epidermal sheet remained static. Three-color live imaging distinguished K14+ epidermal cells (yellow), p63+ epidermal precursor cells (magenta), and dermal cells (cyan) within the hair peg and adjacent epidermal sheet (Fig. S2, Movie S5A, B). As seen in static confocal images, p63 positive cells were noted within the epidermal sheet as well as the epidermal stalk of the hair peg. Several strongly-positive p63 cells were present at the leading edge of the epidermal stalk, abutting the dermal cluster and 1-2 cells were consistently noted at the opposite pole of the dermal cluster, a unique position which could suggest an instructive role in directional epidermal downgrowth.

Hair peg-like structure formation in the organoid droplet culture displays spatiotemporal patterning

Large-scale dermal cell patterns within the droplet culture demonstrated a spatiotemporal progression, which initiated at the droplet periphery and advanced towards the center (Fig. 3A). At 24 hours post-plating, dissociated dermal cells remained distributed in a homogeneous layer without a distinct macroscopic pattern. Over the next 12 hours, dermal cells coalesced into long undulating stripes of higher dermal cell density. By 48 hours in culture, long stripes had subdivided into shorter stripes and, over time, short stripes became rounded, CD34-positive dermal clusters (Fig. 2F). Between 72 and 96 hours, hair peg-like structures formed (Fig. 3B), first at the droplet periphery. In addition to forming earliest, elongated structures approximating more mature hair peg-like structures formed more densely at the periphery (Fig. 3C, D). Centrally, dermal aggregates were 60% larger in diameter, which correlated with the formation of less mature hair peg-like structures and, in many cases, abnormal aggregates possessing multiple epidermal stalks (Fig. 3D). The formative wave of “long stripe - short stripe - rounded cluster – peg-like structure” advanced from the periphery towards the center of the droplet, with each new change in morphology, and the stripe and spot patterns are reminiscent of the periodic patterns predicted by Turing activator-inhibitor principles.[36, 37]

Mathematical modeling simulates the observed spatiotemporal patterns

Reaction-diffusion systems are capable of spontaneously producing sustained spatial patterns. Specifically, spots, stripes and labyrinthine patterns are all possible within the framework of diffusion-driven instability, known as Turing patterns. Once formed, generally only one of these patterns is selected and remains fixed.[38] In contrast, in our droplet culture, multiple distinct patterns occur simultaneously

and are formed in serial progression at different locations within the droplet. As mentioned, such patterning complexity can arise from several different sources. We chose to use a reaction-diffusion description because the transition between spots and stripes is well understood.[38, 39] Critically, in two dimensions, Turing patterns can produce spots and/or stripes, but typically not at the same time.[21] It is simply the competition between the quadratic and cubic terms of the activator kinetics that determine which pattern mode is obtained.[21] Thus, if the correct pattern kinetics are chosen to produce in phase, or out of phase, concentration patterns, then any Turing system can be guided to give rise to spots and/or stripes. Further, a parameter's influence is extremely local in Turing patterns.[22] Thus, all we require to convert a system from spots to stripes is to use a gradient that influences the competition between the cubic and quadratic term. Hence, this is a completely general and robust mechanism for producing such dynamics. Based on this, we propose that an asymmetric spatiotemporal gradient is present to explain the mixed spectrum of patterns within the space (organoid droplet) and the transition of patterns over time. The work implies that the droplet represents an asymmetric morphogenetic field. Indeed, in embryonic development, hairs and feathers form in propagative waves in different body domains, rather than simultaneously.[40-42] This gave us the motivation to develop a simulation of Turing patterning occurring in an asymmetric morphogenetic field (Fig. 3E).

To make the simulation model more broadly applicable, we purposely assigned the morphogens generic activator or inhibitor functions, rather than focusing on specific signaling molecules (please refer to the supplemental methods for a more detailed description). Critically, this work is not about specifying the exact underlying kinetics. Indeed, we do not have sufficiently detailed information to determine the system to this accuracy. The specific use of our model is to highlight that the transition seen in the experiments can be captured, quite generally, using a simple radially symmetric, linear, time dependent gradient. The observed result could be obtained in an infinite number of more complicated ways. However, our results have put a lower bound limit on the complexity required to make a model consistent with the observed results.

Since we observe that hair peg-like structures first form in the periphery, the asymmetry suggests that the activator becomes increasingly sensitive to the inhibitor morphogen v, at the periphery, or, alternatively, the activator becomes decreasingly sensitive to the activator's self-activation response. Such a gradient can easily arise as the experimental droplet is anisotropic, and could be due to chemical signaling (e.g. growth factors) or physical forces in nature, or both. Thus, the principles of Turing activator and inhibitor remain the same, but in different regions we anticipate the field can be heterogeneously predisposed with parameters that favor or suppress periodic patterning. As time progresses, the gradient

increases toward the periphery (bottom simulations of figure "simulation"), and patterns transit from labyrinthine stripes to spots (top simulations of figure "simulation) (Fig. 3E). The spatiotemporal heterogeneity is modeled as a linear spatial gradient that increases at the droplet boundary and fixes over time (Fig. 3E, Movie S6). The visualization of the gradient exhibits itself as a hair peg formative wave traveling from the periphery towards the center of the field, matching experimental results observed in the droplet cultures. Critically, the proposed asymmetry could be wrapped up inside the equations, but this would obscure the essential requirement of a spatio-temporal gradient appearing. Thus, we choose to be explicit with the addition of such complexity.

A platform to modulate hair peg morphogenesis in vitro

To increase the number of hair peg-like structures and to stimulate development beyond the hair peg stage, we modulated multiple parameters within the droplet culture system. The greatest number of hair peg-like structures per droplet culture was generated with a 150 ul volume droplet, 5% FBS concentration, and epidermal to dermal cell ratio of 2:3 (Fig. 4A). An average of 286 hair peg-like structures (±138) per cm^2 with an interfollicular distance of 350 µm was produced under optimal conditions (Fig. 4B). For comparison, endogenous hair pegs from 17 week fetal scalp are spaced, on average, 235 µm apart. The *in vitro* hair peg-like structures were similar in overall shape to hair pegs of 17 week fetal scalp but exhibited significantly different structural proportions. The reconstituted hair peg-like structures possessed shorter, narrower keratinocyte stalks and wider dermal caps while the height of the dermal cap remained consistent with endogenous fetal hair pegs (Fig. 4B). Native fetal scalp exhibited hair pegs of various epidermal stalk heights. The reconstituted hair peg-like structures were, on average, shorter than the endogenous hair pegs but more closely resembled the shorter, early hair pegs in native skin, suggesting that, according to normal developmental patterns, the reconstituted hair peg-like structures could be expected to elongate further before transitioning to the bulbous peg stage. However, our reconstituted hair peg-like structures failed to progress further when they were maintained for three additional days in culture. Clearly, other factors are required.

Although we have not been able to achieve more mature hair follicle formation, the self-organization of periodically arranged hair peg-like structures from dissociated cells is a remarkable process. Detailed analysis of the process enables this droplet culture to serve as a platform for large-scale screening of experimental conditions to optimize *in vitro* follicle formation. We identified four possible signals that might support developmental progression: 1) increased dermal signaling for epidermal downgrowth (Shh, Tgfβ2), 2) stronger dermal papilla inductivity (Wnt7a, FGF2), 3) inhibition of premature

keratinocyte differentiation (protein kinase C (PKC), Noggin, retinoic acid receptors (RAR)), and 4) stimulation of keratinocyte differentiation and/or stratification (FGF2, FGF7/10). [43-50]

Exogenous growth factors were added to the culture medium every 24 hours. A range of concentrations was tested for each protein; results for the concentration which produced the greatest effect are shown (Fig. 4C). Thus far, none of the added factors have resulted in progression to the next stage, the bulbous hair peg. However, a detailed analysis of dermal cap and epidermal stalk width, height, and area identified significant changes mediated by the added growth factors, which, with more investigation, may hold the key to stimulating true follicle formation in culture. Cap and stalk sagittal areas maintained a linear relationship with the total cap and stalk volumes, emphasizing the radial symmetry of these structures and allowing us to simplify analysis by measuring the area of each structure at the midpoint corresponding to maximal width (Fig. S3). During the early peg to bulbous peg transition, the dermal cap becomes more compact and is encapsulated by the base of the elongating epidermal sheath.[30] The addition of 1 µM Shh stimulated epidermal downgrowth, resulting in longer epidermal stalks, as well as a change in the dermal cap shape, with an increased width and cap-stalk overlap, suggesting that Shh may stimulate dermal cell migration proximally along the epidermal stalk or, conversely, epidermal stalk displacement of dermal cap cells (Fig. 4C). The protein kinase C inhibitors, chelerythrine chloride and bisindolylmaleimide I, produced a similar effect, with increased epidermal stalk length and overall stalk area, as well as increased dermal cap area and cap-stalk overlap. FGF2, in combination with Shh, decreased dermal cap height and area and the retinoic acid receptor antagonist ER50891 enhanced total stalk area. Though subtle changes were evident when exogenous factors were added, they were insufficient to alter the gross morphology of the hair peg-like structure and push development into the bulbous peg stage.

Discussion

The ability to tissue engineer human hair follicles for transplantation would eliminate a treatment gap for numerous patients. Over the years, our group's research has focused on the morphogenesis of skin appendages. Recently, we examined the self-organizing behavior of dissociated epidermal and dermal newborn mouse cells and their ability to reconstitute functional follicles.[4] Similar studies of human follicular morphogenesis have been difficult to achieve, due to the low efficiency of follicle formation from readily-available adult cells and the long time to follicle formation. Here, we demonstrated the production of human hair peg-like structures *in vitro* from a well-defined mixture of progenitor cells. In this three-dimensional organoid droplet culture, dissociated neonatal epidermal and fetal dermal cells progressed, via self-organization, through the following reproducible and recognizable stages akin to early follicle development to reach cellular configurations similar to hair pegs *in situ*: (1) mixed dissociated cells, (2) cell sheets, (3) dermal stripes and clusters, (4) dermal clusters with associated epidermal placode-like collections, and (5) distinct hair peg-like structures with spatial periodicity.[30] The developmental process proceeded rapidly within 96 hours and was dependent on epidermal:dermal cell ratio and factor concentration, suggesting the need for an appropriate balance of epithelial-mesenchymal signaling factors or cell-cell interactions. This *in vitro* culture system demonstrates the initiation and rapid progression of early stages of human follicle-like development. It also shows that human and mouse cells utilize different morphogenetic paths in the morphospace of epidermal-dermal multicellular configurations and may explain why it has been difficult to achieve robust human hair reconstitution. We hypothesize that the differences between human and mouse hair follicle reconstitution may be due to three factors: *epidermal cell plasticity, the inducing ability of dermal cells, and morphogenetic field competence*.

1) The plasticity of foreskin keratinocytes is known to wane with prolonged culture, resulting in reduced hair follicle formation.[51] We hypothesized that a loss of epidermal plasticity inhibited further follicle organoid development *in vitro* beyond the peg stage. Protein kinase C (PKC) and retinoic acid pathways play a role in epidermal differentiation and stratification during skin development. Excessive retinoic acid causes cessation of hair follicle development at the germ stage in mice, while inhibition of PKC promotes folliculogenesis from adult mouse cells.[4, 47, 49] The addition of PKC inhibitors and an RAR antagonist exhibited positive effects on the length and diameter of the epidermal stalk but was insufficient to drive further folliculogenesis, suggesting that other factors are required for progressive development. We suspect that the less primitive epigenetic state of the keratinocytes used may be the molecular basis

for suboptimal competence. In future studies, we will search for factors that can "reprogram" these keratinocytes or use more responsive keratinocytes.

2) The inducing ability of dermal cells is a second critical component for folliculogenesis. The dermal papilla releases multiple factors, which participate in epidermal-mesenchymal signaling during folliculogenesis. Shh and Tgfβ are necessary for epidermal downgrowth and mice which lack Shh signaling possess hair follicles which are stalled at the germ/peg stage.[43, 44] The addition of Shh to the droplet cultures stimulated additional epidermal downgrowth but did not cause structural progression to the bulbous peg stage. We also examined Wnt7a and FGF2, which have been shown to maintain proliferation and inductivity in cultured murine dermal papilla cells.[45, 46] Yet, we did not observe significant progress in organoid development. The dermal papilla-like cells in our culture do not appear fully functional as they can only support the induction of hair peg-like structures, not mature follicles. However, this system provides a promising platform for the continued search for factors or conditions which enhance inductivity.

3) The morphogenetic field, comprised of epidermal cells, dermal cells and extracellular matrix together, must enter a competent stage for periodic patterning to begin. The developing embryo is a heterogeneous morphogenetic field with anisotropic growth in which chemical factors, cell types, and mechanical forces are unevenly distributed in three spatial dimensions and one temporal dimension. Here, our organoid culture demonstrates obvious asymmetry within the droplet, as patterns began at the periphery and migrated centrally. Labyrinthine stripes of dermal cells were noted initially, which subsequently transformed into periodically arranged dermal cell clusters. Both stripes and dermal clusters can be produced by a simple Turing model and can reflect an intermediate stage of the final periodic patterns if there is an uneven morphogenetic field.[38] What can account for the difference in progression through the periodic patterning process? While a simple generic radial gradient effected by one component may be sufficient for a Turing activator-inhibitor system to produce the pattern here, it may not be sufficient to produce the complex spatiotemporal patterning transitions we observed experimentally.[36, 37] Here, we purposely designed a generic model, to have wider conceptual application. Simulation with mathematical modeling suggests similar patterning sequences can be achieved through uneven chemical signaling activities[52] (e.g., higher concentration of activator morphogens at the droplet periphery or higher sensitivity of cells at the droplet periphery) or uneven mechanical forces[53] (e.g., cellular tension or matrix rigidity favor periodic formation at the droplet periphery). The mathematical and experimental models presented here will help us identify the molecular basis of these patterning processes in the analyzable droplet *in vitro* and in the complex developing embryo *in vivo* in the future.

In vivo, chicken feather buds form exquisite hexagonal patterns progressively from the midline to the flank. Earlier works have suggested this results from a local Turing event and a global propagating event.[54] However, the nature of the global even is unknown. This is part of the motivation for this study, to use the organoid droplet to understand more about the nature of the sequential appearance of hair or feather primordia. It is timely that a paper reporting a global Eda wave spreading from the midline to the flank is just reported, which suggests Eda induces FGF20, followed by dermal cell aggregate formation, thus facilitating Turing patterning via mechano-chemical coupling.[55] Based on this and other studies, we propose a new integrated understanding that a Turing periodic patterning occurs with or without a global propagation mechanism. The global mechanism can be chemical or mechanical in nature, as long as it can tilt the Turing activator / inhibitor system ratio.[56] The asymmetric morphogenetic field in the organoid culture studied here presents a good model to further test how this global asymmetry mechanism works.

With two cellular components, the initial epidermal and dermal cell ratio will influence the final stable position in the morpho-space of two-component multi-cellular assemblies.[4] The initial conditions, determined by the probability of cell collision and the relative strength of cell adhesion, control the initial multi-cellular configuration. In the human cell culture droplet, epidermal-matrix adhesions appear to dominate, leading to the formation of the epidermal layer first. Dermal-dermal interactions are stronger than epidermal-dermal adhesions, leading to the formation of dermal stripes and dermal clusters. However, during morphogenetic processes, there can be “qualitative changes” of cellular collectives. Following the formation of dermal condensations, epidermal-dermal condensate adhesion increases and can induce the formation of hair peg-like structures, up to the extent that epidermal basement membrane polarity is reversed. Thus, the high resolution analysis of the process of hair peg formation provides an excellent opportunity to fine tune key cellular events.

In summary, we have demonstrated that human fetal scalp dermal cells, in association with competent epidermal cells, can direct the rapid regeneration of human hair peg-like organoids *in vitro*. The opportunity to study the asymmetric spatiotemporal sequence of periodic patterning within the droplet provides insights into the self-organizing behavior of skin progenitor cells. Furthermore, this *in vitro* culture system provides an opportunity to study ways to restore and optimize hair follicle regeneration from easily-obtainable adult dermal cells and may support the production of complete hair follicles for transplantation in the future.

Acknowledgements

This work was supported by funding from the American College of Surgeons (E.L.W.), the California Institute for Regenerative Medicine (E.L.W.), the A. P. Giannini Foundation (E.L.W.), a graduate fellowship from the Ministry of National Defense of Taiwan (K.L.O.), the L. K. Whittier Foundation (C.M.C.), the National Institute of Arthritis and Musculoskeletal and Skin Diseases of the National Institutes of Health (AR 47364, AR 60306; and GM125322 to C.M.C.), and the National Science Foundation (DMS1440386 to T.E.W. and P.K.M.). We thank Dr. Chin Lin Guo for helpful discussion and acknowledge the USC Research Center for Liver Disease Cell and Tissue Imaging Core and the USC Stem Cell Microscopy Core Facility for their assistance and participation. We thank Dr. R.B. Widelitz for helpful input. T.E.W. and P.K.M. thank the Mathematical Biosciences Institute (MBI) at Ohio State University for helping to initiate this research. MBI receives its funding through the National Science Foundation grant DMS1440386.

Author contributions

E.L.W. and C.M.C. conceived the idea and experimental design. E.L.W. and K.L.O. conducted the experiments. C.Y.Y. provided imaging expertise. T.E.W. and P.K.M. produced mathematical modeling. E.L.W., T.E.W. and C.M.C. prepared the manuscript.

Competing Interests

The authors declare no competing financial interests.

References

[1] M. Takeo, T. Tsuji, Curr. Opin. Genet. Dev. 2018, 52, 42.

[2] Y. Zheng, X. Du, W. Wang, M. Boucher, S. Parimoo, K. Stenn, J. Invest. Dermatol. 2005, 124, 867.

[3] L. F. Lee, T. X. Jiang, W. Garner, C. M. Chuong, Tissue Eng. Part C Methods 2011, 17, 391.

[4] M. Lei, L. J. Schumacher, Y. C. Lai, W. T. Juan, C. Y. Yeh, P. Wu, T. X. Jiang, R. E. Baker, R. B. Widelitz, L. Yang, C. M. Chuong, Proc. Natl. Acad. Sci. U. S. A. 2017, 114, E7101.

[5] C. A. Higgins, J. C. Chen, J. E. Cerise, C. A. Jahoda, A. M. Christiano, Proc. Natl. Acad. Sci. U. S. A. 2013, 110, 19679.

[6] R. L. Thangapazham, P. Klover, J. A. Wang, Y. Zheng, A. Devine, S. Li, L. Sperling, G. Cotsarelis, T. N. Darling, J. Invest. Dermatol. 2014, 134, 538.

[7] X. Wu, L. Scott, Jr., K. Washenik, K. Stenn, Tissue Eng. Part A 2014, 20, 3314.

[8] Q. Zhang, T. Zu, Q. Zhou, J. Wen, X. Leng, X. Wu, Regen. Med. 2017, 12, 503.

[9] H. E. Abaci, A. Coffman, Y. Doucet, J. Chen, J. Jackow, E. Wang, Z. Guo, J. U. Shin, C. A. Jahoda, A. M. Christiano, Nat. Commun. 2018, 9, 5301.

[10] J. Lee, R. Bscke, P. C. Tang, B. H. Hartman, S. Heller, K. R. Koehler, Cell Rep. 2018, 22, 242.

[11] K. E. Toyoshima, K. Asakawa, N. Ishibashi, H. Toki, M. Ogawa, T. Hasegawa, T. Irie, T. Tachikawa, A. Sato, A. Takeda, T. Tsuji, Nat. Commun. 2012, 3, 784.

[12] R. Takagi, J. Ishimaru, A. Sugawara, K. E. Toyoshima, K. Ishida, M. Ogawa, K. Sakakibara, K. Asakawa, A. Kashiwakura, M. Oshima, R. Minamide, A. Sato, T. Yoshitake, A. Takeda, H. Egusa, T. Tsuji, Sci. Adv. 2016, 2, e1500887.

[13] J. J. Velazquez, E. Su, P. Cahan, M. R. Ebrahimkhani, Trends Biotechnol. 2018, 36, 415.

[14] S. C. Chueh, S. J. Lin, C. C. Chen, M. Lei, L. M. Wang, R. Widelitz, M. W. Hughes, T. X. Jiang, C. M. Chuong, Expert Opin. Biol. Ther. 2013, 13, 377.

[15] P. K. Maini, R. E. Baker, C. M. Chuong, Science 2006, 314, 1397.

[16] R. Sennett, M. Rendl, Semin. Cell Dev. Biol. 2012, 23, 917.

[17] S. Kondo, T. Miura, Science 2010, 329, 1616.

[18] A. Nakamasu, G. Takahashi, A. Kanbe, S. Kondo, Proc. Natl. Acad. Sci. U. S. A. 2009, 106, 8429.

[19] J. D. Murray, P. K. Maini, R. T. Tranquillo, Physics Reports 1988, 171, 59.

[20] A. M. Turing, Philos. Trans. R. Soc. Lond. B. Biol. Sci. 1952, 237, 37.

[21] H. Meinhardt, Interface Focus 2012, 2, 407.

[22] T. X. Jiang, R. B. Widelitz, W. M. Shen, P. Will, D. Y. Wu, C. M. Lin, H. S. Jung, C. M. Chuong, Int. J. Dev. Biol. 2004, 48, 117.

[23] C. M. Chuong, C. Y. Yeh, T. X. Jiang, R. Widelitz, Wiley Interdiscip. Rev. Dev. Biol. 2013, 2, 97.

[24] H. C. Chiu, C. H. Chang, J. S. Chen, S. H. Jee, J. Formos. Med. Assoc. 1996, 95, 667.

[25] C. A. Higgins, G. D. Richardson, D. Ferdinando, G. E. Westgate, C. A. Jahoda, Exp. Dermatol. 2010, 19, 546.

[26] K. Inoue, N. Aoi, Y. Yamauchi, T. Sato, H. Suga, H. Eto, H. Kato, Y. Tabata, K. Yoshimura, J. Cell. Mol. Med. 2009, 13, 4643.

[27] C. A. Jahoda, A. J. Reynolds, C. Chaponnier, J. C. Forester, G. Gabbiani, J. Cell Sci. 1991, 99 (Pt 3), 627.

[28] Y. Miao, Y. B. Sun, B. C. Liu, J. D. Jiang, Z. Q. Hu, Tissue Eng. Part A 2014, 20, 2329.

[29] K. Yamauchi, A. Kurosaka, Arch. Dermatol. Res. 2009, 301, 357.

[30] R. Paus, S. Muller-Rover, C. Van Der Veen, M. Maurer, S. Eichmuller, G. Ling, U. Hofmann, K. Foitzik, L. Mecklenburg, B. Handjiski, J. Invest. Dermatol. 1999, 113, 523.

[31] L. Ahtiainen, S. Lefebvre, P. H. Lindfors, E. Renvoise, V. Shirokova, M. K. Vartiainen, I. Thesleff, M. L. Mikkola, Dev. Cell 2014, 28, 588.

[32] T. Andl, S. T. Reddy, T. Gaddapara, S. E. Millar, Dev. Cell 2002, 2, 643.
[33] D. L. Gay, C. C. Yang, M. V. Plikus, M. Ito, C. Rivera, E. Treffeisen, L. Doherty, M. Spata, S. E. Millar, G. Cotsarelis, J. Invest. Dermatol. 2015, 135, 45.
[34] J. Huelsken, R. Vogel, B. Erdmann, G. Cotsarelis, W. Birchmeier, Cell 2001, 105, 533.
[35] C. G. Schirren, W. H. Burgdorf, C. A. Sander, G. Plewig, Am. J. Dermatopathol. 1997, 19, 335.
[36] C. M. Lin, T. X. Jiang, R. E. Baker, P. K. Maini, R. B. Widelitz, C. M. Chuong, Dev. Biol. 2009, 334, 369.
[37] S. Kondo, J. Theor. Biol. 2017, 414, 120.
[38] B. Ermentrout, Proceedings of the Royal Society of London. Series A: Mathematical and Physical Sciences 1991, 434, 413.
[39] A. L. Krause, V. Klika, T. E. Woolley, E. A. J. P. R. E. Gaffney, Phys. Rev. E 2018, 97, 052206.
[40] Y. Wang, H. Chang, J. Nathans, Development 2010, 137, 4091.
[41] B. Gworys, Z. Domagala, Ann. Anat. 2003, 185, 383.
[42] P. Sengel, A. Mauger, Dev. Biol. 1976, 51, 166.
[43] B. St-Jacques, H. R. Dassule, I. Karavanova, V. A. Botchkarev, J. Li, P. S. Danielian, J. A. McMahon, P. M. Lewis, R. Paus, A. P. McMahon, Curr. Biol. 1998, 8, 1058.
[44] K. Foitzik, R. Paus, T. Doetschman, G. P. Dotto, Dev. Biol. 1999, 212, 278.
[45] J. Kishimoto, R. E. Burgeson, B. A. Morgan, Genes Dev. 2000, 14, 1181.
[46] A. Osada, T. Iwabuchi, J. Kishimoto, T. S. Hamazaki, H. Okochi, Tissue Eng. 2007, 13, 975.
[47] C. S. Harmon, T. D. Nevins, W. B. Bollag, Br. J. Dermatol. 1995, 133, 686.
[48] V. A. Botchkarev, N. V. Botchkareva, A. A. Sharov, K. Funa, O. Huber, B. A. Gilchrest, J. Invest. Dermatol. 2002, 118, 3.
[49] J. Okano, C. Levy, U. Lichti, H. W. Sun, S. H. Yuspa, Y. Sakai, M. I. Morasso, J. Biol. Chem. 2012, 287, 39304.
[50] X. J. Zhu, Y. Liu, Z. M. Dai, X. Zhang, X. Yang, Y. Li, M. Qiu, J. Fu, W. Hsu, Y. Chen, Z. Zhang, PLoS Genet. 2014, 10, e1004687.
[51] R. L. Thangapazham, P. Klover, S. Li, J. A. Wang, L. Sperling, T. N. Darling, Exp. Dermatol. 2014, 23, 443.
[52] J. D. Glover, K. L. Wells, F. Matthaus, K. J. Painter, W. Ho, J. Riddell, J. A. Johansson, M. J. Ford, C. A. B. Jahoda, V. Klika, R. L. Mort, D. J. Headon, PLoS Biol. 2017, 15, e2002117.
[53] A. E. Shyer, A. R. Rodrigues, G. G. Schroeder, E. Kassianidou, S. Kumar, R. M. Harland, Science 2017, 357, 811.
[54] T. X. Jiang, H. S. Jung, R. B. Widelitz, C. M. Chuong, Development 1999, 126, 4997.
[55] W. K. W. Ho, L. Freem, D. Zhao, K. J. Painter, T. E. Woolley, E. A. Gaffney, M. J. McGrew, A. Tzika, M. Milinkovitch, P. Schneider, A. Drusko, F. Matthäus, J. L. Glover, K. L. Wells, J. A. Johansson, M. G. Davey, H. M. Sang, M. Clinton, D. J. Headon, PLoS Biol. in press.
[56] M. Inaba, H. I.-C. Harn, C. M. Chuong, PLoS Biol. in press.
[57] Y. Soneoka, P. M. Cannon, E. E. Ramsdale, J. C. Griffiths, G. Romano, S. M. Kingsman, A. J. Kingsman, Nucleic Acids Res. 1995, 23, 628.

Figure Legends

Figure 1. Human neonatal foreskin keratinocytes and fetal scalp dermal cells self-organized to form hair peg-like structures *in vitro*.

A. Schematic of the *in vitro* hair follicle reconstitution assay. Follicular organoids, composed of epidermal (green) and dermal cells (red), protrude from a multi-layered keratinocyte sheet (green). hNFKs = human neonatal foreskin keratinocytes, hFSDs = human fetal scalp dermal cells.

B. Serial brightfield and confocal images of the culture droplet taken every 24 hours demonstrated the formation of periodically arranged three-dimensional configurations by 96 hours, corresponding to hair peg-like structures composed of an epidermal stalk and dermal cap. Whole mount confocal images in the second and third rows, with pancytokeratin denoting epidermal cells in green and nuclei in red, were taken from the periphery of the droplet, as represented by the white dotted box in the brightfield image in the first row. In the second row, the white dotted line demarcates the periphery of the droplet. The fourth row of images are triple-stained sections, with pancytokeratin (panCK) marking epidermal cells (green), vimentin marking dermal cells (red), and nuclei (blue) stained with TO-PRO-3 iodide. The scale bar is the same for all images per row. The large green lobules in the 48 hours sample are dead cell artifacts which have trapped the fluorescent antibody. (n=25)

C. *In vitro* structures at 96 hours (left panel) resembled hair pegs found in 19 week human fetal scalp (right panel). p63 is a marker of epidermal progenitor cells. (n=25)

D. Human fetal scalp dermal cells alone and adult scalp dermal cells mixed with neonatal foreskin keratinocytes did not produce any hair peg-like structures after 96 hours in culture. The images are taken from the periphery of the culture droplet, as exemplified by the black dotted box in B. hASDs = human adult scalp dermal cells.

E. When injected subcutaneously into a nude mouse, human neonatal foreskin keratinocytes and fetal scalp dermal cells produced mature hair follicles composed of cells of human origin. Pancytokeratin (green) and vimentin (cyan) antibodies are human-specific. Sections of mouse skin were included to confirm species-specificity of the antibodies (bottom panels). (n=3)

Figure 2. Hair peg-like structures formed *in vitro* expressed appropriate epidermal and dermal markers and progressed through reproducible stages reminiscent of early hair follicle development.

A. Staining of sections of hair peg-like structures with keratin-14 (green) demonstrated clear separation between epidermal and dermal cells (top left). Consistent with patterns of keratin expression in human fetal scalp, epidermal cells within the *in vitro* hair peg-like structures did not express keratin-10 (red). Involucrin (green), a marker of keratinocyte terminal differentiation, was highly expressed in only a portion of the epidermal sheet, which, along with keratin-10 expression, suggests stratification (bottom left). Involucrin also strongly marked cells believed to be terminally-differentiated, anuclear corneocytes that became inappropriately trapped within the dermal cell cap. The epidermal stalks were keratin-17 (green), keratin-18 (magenta), and E-cadherin (green) positive (whole mount, top right). Several of the larger hair peg-like structures appeared to have epidermal stalks with central lumens and concentrically organized keratinocytes, marked by keratin 14 (green) (whole mount, bottom right).

B. At 24 hours, all keratinocytes expressed p63 (green), a marker of epidermal stemness (sections, top panel). By 72 and 96 hours, p63 positive cells were localized to the basal layer of the epidermal sheet and the leading edge of the epidermal stalk abutting the dermal cap (middle panel). 96-hour images are whole mount specimens. PCNA-positive (green), actively proliferating cells were present within the basal layer of the epidermal sheet, the epidermal stalk at the interface with the dermal cap, and the periphery of the dermal cap, similar to 17-week second trimester human fetal scalp (sections, bottom panel).

C. The cells of the dermal cap expressed collagen I (green, section and whole mount) and collagen III (green, whole mount) (top left). K10 = keratin-10. Collagen IV (red) and laminin-332 (green), markers of the dermal papilla basement membrane, were expressed at the interface between epidermal and dermal cells within the hair peg-like structures *in vitro* (whole mount, bottom left). PanCK = pancytokeratin, nuc = nuclei, vim = vimentin. α-SMA (green), a marker of human dermal papilla cells in culture, was expressed within the center of the dermal cap (whole mount, top right). Human dermal papilla cells *in vivo* express alkaline phosphatase (alk phos (green), left image), a marker which is typically lost during *in vitro* culture. The dermal cap was also positive or versican, a commonly-used dermal condensate or dermal papilla marker (whole mount, bottom right).

D. Serial optical sections of a dermal aggregate at 48 hours imaged at increasing droplet depths demonstrated a rounded, dense dermal cluster atop an epidermal sheet with concentrically-arranged nuclei, reminiscent of the epidermal placode.

E. β-catenin was expressed throughout the epidermal sheet at 48 hours but was restricted to those epidermal cells associated with the dermal cap by 72 hours (sections, top panels). Dermal cells within the dermal cap were positive for CD34, a marker of the early dermal papilla stem cell (bottom panels). The 48-hour image is a whole mount specimen. All other images are sections.

All staining was performed on multiple hair peg-like structures from at least three biological replicates. (n=3)

Figure 3. Collectively, a stripe-to-dot formative gradient forms from the center to periphery of the culture droplet and suggests a Turing periodic pattering process on an asymmetric field.

A. Brightfield images of a single culture droplet taken every 12 hours demonstrated the formation of an initial trabecular pattern, which then gave way to the periodically arranged stripes and cell clusters (top row). Line drawings created from brightfield images (middle row) and a schematic where red represents dermal cells and green represents epidermal cells (bottom row) emphasize the transitions in distinct periodic patterns as they relate to developmental stages. (n=4)

B. High-power magnification demonstrates the hair peg-like architecture under brightfield imaging. (n=4)

C. The field was divided into five concentric zones. Anatomic hair peg-like structures developed at a higher density in zones 4-5, toward the periphery of the droplet. In paired t-test comparisons, the average density of hair peg-like structures at the periphery of the culture droplet was statistically different from more central zones (*$p<0.05$). Error bars represent standard error of the mean. (n=11)

D. Dermal clusters of a smaller diameter were more likely to be associated with single stalked hair peg-like structures than were larger dermal clusters found at the center of the droplet. Average cluster diameter is plotted. Paired t-test comparisons were used to examine statistically significant differences between groups. Error bars represent standard error of the mean. *$p<0.05$, **$p<0.01$. (n=3)

E. Numerical simulations of reaction-diffusion equations are presented in the methods section. The top row illustrates how the density of activator (u) alters over time, with darker colors presenting high density regions and lighter colors representing low density regions. The bottom row illustrates the radially symmetric spatiotemporal gradient field that alters the properties of the reaction-diffusion equations heterogeneously across the domain. As time increases, the value of the field at the boundary increases to a maximum value and the gradient gets steeper. We see that as the gradient steepens, the activator pattern transitions from spots at the periphery to labyrinthine patterns in the center, which recapitulates the *in vitro* periodic patterns. Additional parameter values are given in Table S3.

Figure 4. **Modulation of hair peg morphogenesis *in vitro*.**

A. Here, we examine the conditions that can influence the number, size and progression of the hair peg-like structures. Hair peg-like structures formed more frequently when culture medium contained 5% FBS and when an epidermal to dermal cell ratio of 2:3 was used. The average number of hair peg-like structures formed per condition is plotted, with error bars representing standard error of the mean and statistical significance assessed with paired t-tests. *p<0.05. (n=6)

B. The *in vitro* hair peg-like structures (black bars) show similar architecture to hair pegs in 17 week human fetal scalp (gray bars). However, the average stalk height, stalk width, and cap width of the *in vitro* hair peg-like structures were significantly smaller. While the *in vitro* hair peg-like structures formed at regular intervals, there was a larger average inter-follicular distance than is found in fetal scalp tissue. An asterisk denotes a p-value of < 0.05, when compared to native human fetal scalp, via paired t-tests. Error bars represent standard error of the mean. (n=5)

C. The addition of growth factors to the droplet cultures caused significant changes in certain aspects of the epidermal stalk and dermal cap dimensions, but did not induce further development into a bulbous peg structure. Dimensions measured: 1) epidermal stalk width, 2) epidermal stalk length, 3) epidermal stalk area at the structure midpoint, 4) dermal cap width, 5) dermal cap height, 6) epidermal stalk-dermal cap overlap, and 7) dermal cap area at the structure midpoint. Growth factors: A) negative control, B) Shh 1 µg/ml, C) Tgfβ2 0.5 µg/ml, D) RAR antagonist ER50891 1 µM, E) FGF7 + FGF10 1 µg/ml, F) FGF2 1 µg/ml, G) FGF2 + Shh 1 µg/ml, H) FGF2 + Wnt7a 1 µg/ml, I) PKCi 660 nM chelerythrine chloride and 10 nM bisindolylmaleimide I, and J) Noggin 1 µg/ml. All measurements were normalized to the negative control and average dimensions are shown. Error bars represent standard error of the mean. Statistical significance between two groups was calculated using paired t-tests. An asterisk denotes a p-value < 0.05, compared to the negative control without added factors. (n≥3)

Figure 1.

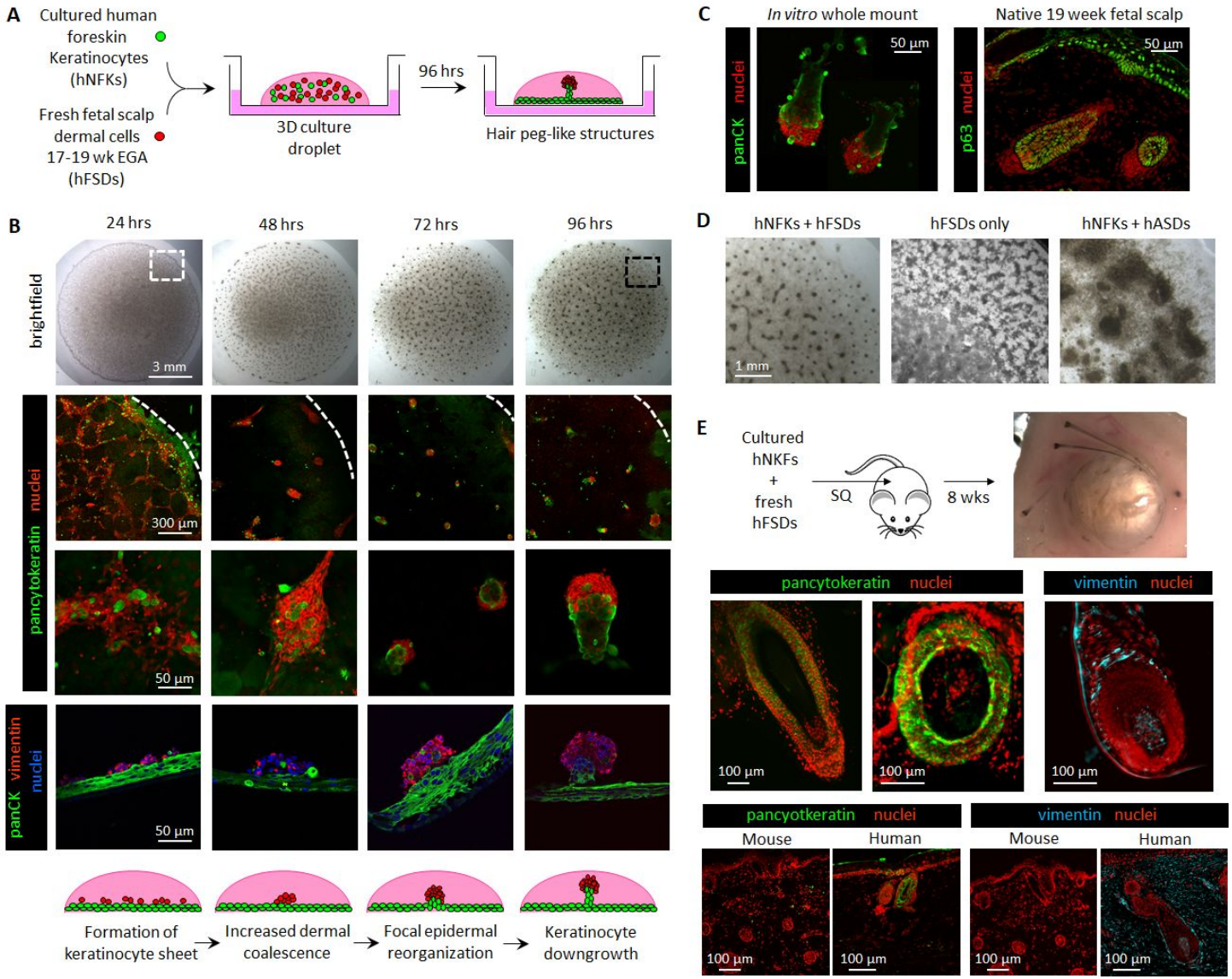
A
Cultured human foreskin Keratinocytes (hNFKs)
Fresh fetal scalp dermal cells 17-19 wk EGA (hFSDs)
3D culture droplet
96 hrs
Hair peg-like structures
B
24 hrs
48 hrs
72 hrs
96 hrs
brightfield
3 mm
pancytokeratin nuclei
300 µm
50 µm
panCK vimentin nuclei
50 µm
Formation of keratinocyte sheet
Increased dermal coalescence
Focal epidermal reorganization
Keratinocyte downgrowth
C
In vitro whole mount
Native 19 week fetal scalp
panCK nuclei
50 µm
p63 nuclei
50 µm
D
hNFKs + hFSDs
hFSDs only
hNFKs + hASDs
1 mm
E
Cultured hNKFs + fresh hFSDs
SQ
8 wks
pancytokeratin nuclei
vimentin nuclei
100 µm
100 µm
100 µm
pancyotkeratin nuclei
vimentin nuclei
Mouse
Human
Mouse
Human
100 µm
100 µm
100 µm
100 µm

Figure 2.

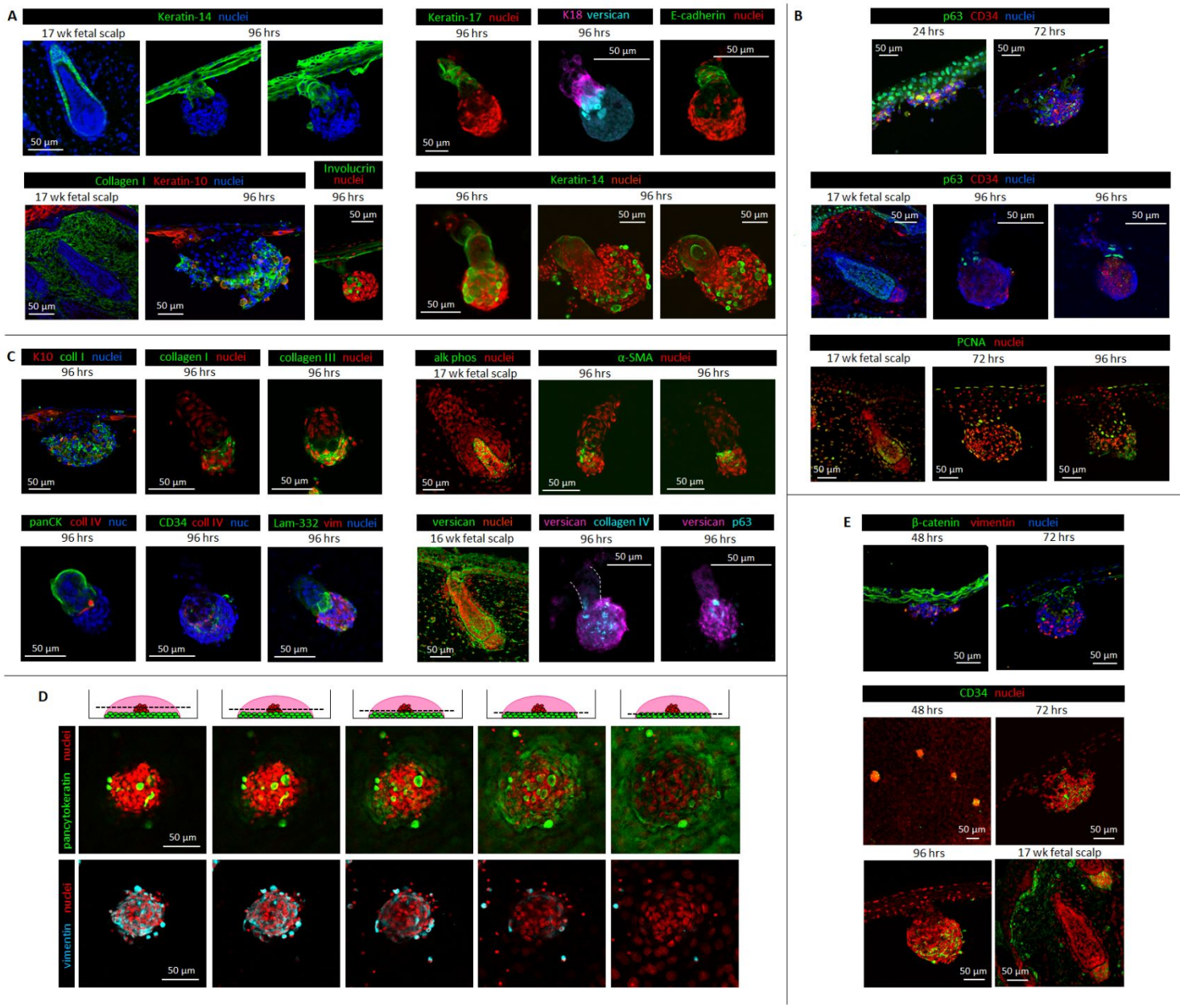
A
Keratin-14 nuclei
17 wk fetal scalp
96 hrs
Keratin-17 nuclei
96 hrs
K18 versican
96 hrs
E-cadherin nuclei
Collagen I Keratin-10 nuclei
17 wk fetal scalp
96 hrs
Involucrin nuclei
96 hrs
Keratin-14 nuclei
96 hrs
96 hrs
B
p63 CD34 nuclei
24 hrs
72 hrs
p63 CD34 nuclei
17 wk fetal scalp
96 hrs
96 hrs
PCNA nuclei
17 wk fetal scalp
72 hrs
96 hrs
C
K10 coll I nuclei
96 hrs
collagen I nuclei
96 hrs
collagen III nuclei
96 hrs
alk phos nuclei
17 wk fetal scalp
α-SMA nuclei
96 hrs
96 hrs
panCK coll IV nuc
96 hrs
CD34 coll IV nuc
96 hrs
Lam-332 vim nuclei
96 hrs
versican nuclei
16 wk fetal scalp
versican collagen IV
96 hrs
versican p63
96 hrs
D
pancytokeratin nuclei
vimentin nuclei
E
β-catenin vimentin nuclei
48 hrs
72 hrs
CD34 nuclei
48 hrs
72 hrs
96 hrs
17 wk fetal scalp
50 μm

Figure 3.

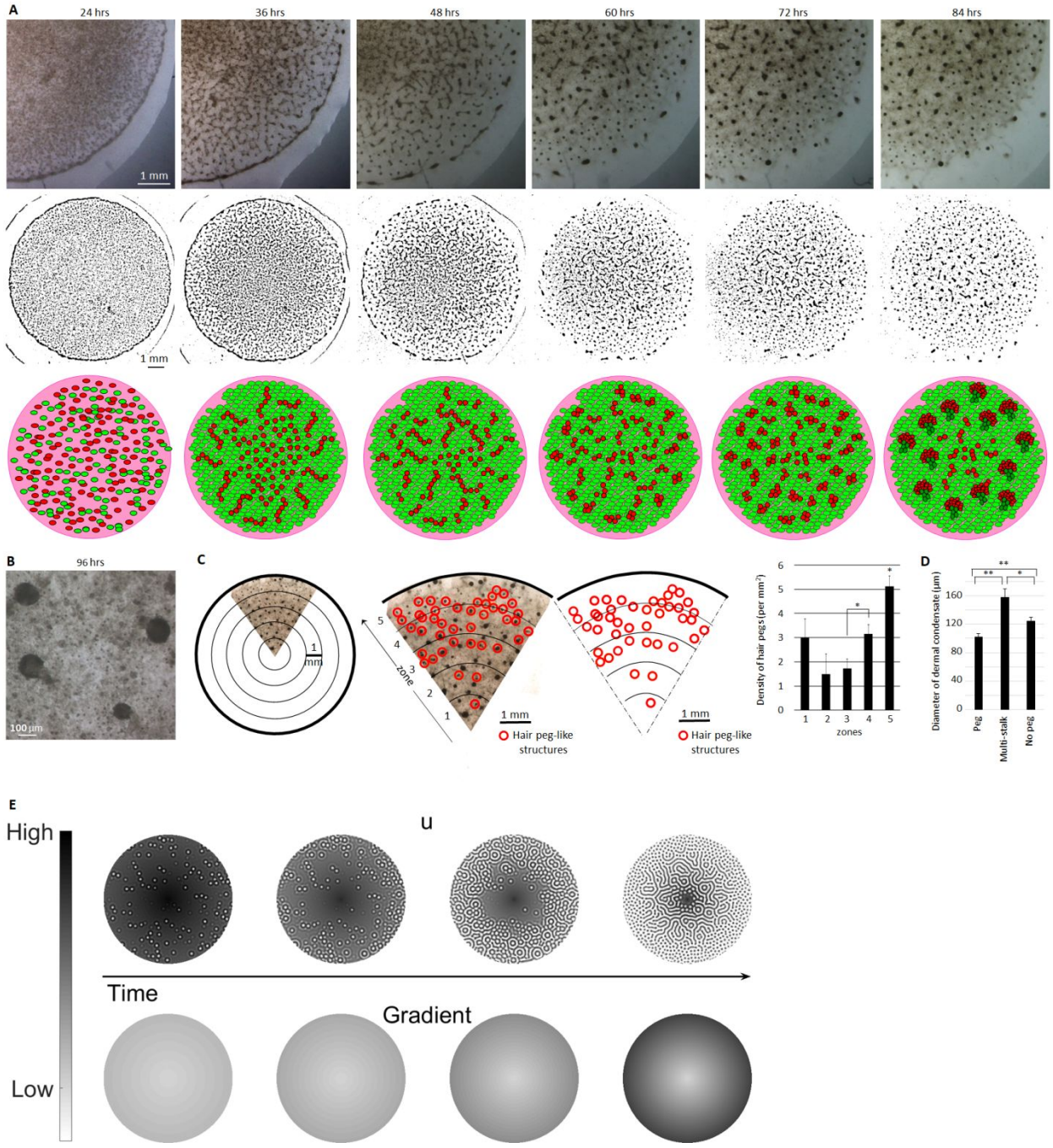
A
24 hrs
36 hrs
48 hrs
60 hrs
72 hrs
84 hrs
1 mm
B
96 hrs
100 µm
C
1 mm
zone
Hair peg-like structures
Density of hair pegs (per mm²)
zones
D
Diameter of dermal condensate (µm)
Peg
Multi-stalk
No peg
E
High
Low
Time
Gradient
u

Figure 4.

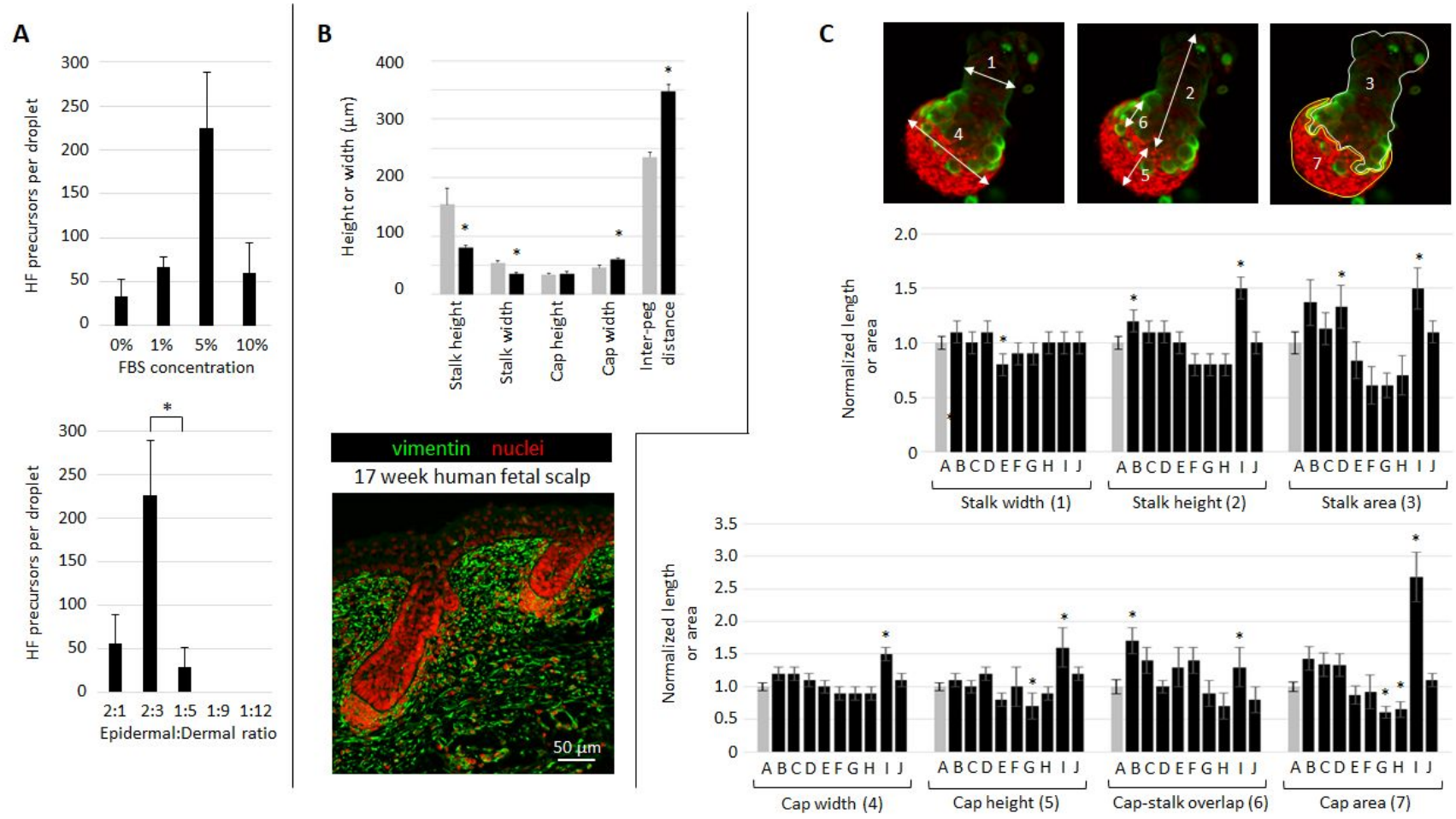
A
HF precursors per droplet
300
250
200
150
100
50
0
0% 1% 5% 10%
FBS concentration
*
HF precursors per droplet
2:1 2:3 1:5 1:9 1:12
Epidermal:Dermal ratio
B
Height or width (µm)
400
300
200
100
0
Stalk height
Stalk width
Cap height
Cap width
Inter-peg distance
vimentin nuclei
17 week human fetal scalp
50 µm
C
1
2
3
4
5
6
7
Normalized length or area
2.0
1.5
1.0
0.5
0
A B C D E F G H I J
Stalk width (1)
Stalk height (2)
Stalk area (3)
3.5
3.0
2.5
2.0
1.5
1.0
0.5
0
Cap width (4)
Cap height (5)
Cap-stalk overlap (6)
Cap area (7)

Supplemental Information

Self-organizing hair peg-like structures from dissociated skin progenitor cells: New insights for human hair follicle organoid engineering and Turing patterning in an asymmetric morphogenetic field

Erin L. Weber, M.D., Ph.D.[1,2]

Thomas E. Woolley, Ph.D.[3]

Chao-Yuan Yeh, M.D.[1]

Kuang-Ling Ou, M.D.[1,4,5]

Philip K. Maini, Ph.D.[6]

Cheng-Ming Chuong, M.D., Ph.D.[1,7,*]

[1] Department of Pathology, Keck School of Medicine of the University of Southern California, Los Angeles, CA

[2] Division of Plastic and Reconstructive Surgery, Keck School of Medicine of the University of Southern California, Los Angeles, CA

[3] Cardiff School of Mathematics, Cardiff University, Senghennydd Road, Cardiff, CF24 4AG, UK.

[4] Ostrow School of Dentistry of the University of Southern California, Los Angeles, CA

[5] Division of Plastic and Reconstructive Surgery, Department of Surgery, Tri-Service General Hospital, National Defense Medical Center, Taipei, Taiwan

[6] Wolfson Centre for Mathematical Biology, Mathematical Institute, Oxford, OX2 6GG, UK.

[7] Integrative Stem Cell Center, China Medical University, Taichung, Taiwan

Corresponding author: Cheng-Ming Chuong, M.D., Ph.D.
Keck School of Medicine of the University of Southern California
2011 Zonal Ave, HMR 313B
Los Angeles, CA 90089
cmchuong@usc.edu

Table of contents:

Supplemental Methods

Tissues and cells

Neonatal foreskin was obtained from the Cooperative Human Tissues Network (Nashville, TN). Second trimester fetal scalp skin, 17-19 weeks estimated gestational age (EGA), was obtained from Novogenix, Inc. (Los Angeles, CA) or Advanced Bioscience Resources (Alameda, CA). The tissues were incubated in 0.5% dispase overnight at 4°C. The epidermis and dermis were then mechanically separated using fine forceps and incubated in 0.35% collagenase I at 37°C for 30 minutes with occasional mixing. FBS was added to stop digestion. The epidermal and dermal cells were released from the surrounding matrix by pipetting with a glass pipette. The cells were passed through a 70 µm filter and centrifuged at 180xg for 5 minutes to remove debris. The epidermal cells were resuspended and cultured in CnT-PR medium (ZenBio) with penicillin, streptomycin, and amphotericin B (P/S/A) on plates treated with Coating Matrix (Life Technologies). Media was replaced every 4 days and cells were split at 80% confluency for a maximum of 4 weeks. The dermal cells were incubated in RBC lysis buffer (154 mM NH_4Cl, 10 mM $KHCO_3$, 0.1 mM EDTA, pH 7.2) at room temperature for 5 minutes and recentrifuged. RBC lysis was repeated once if needed and the cell pellet was washed with 1xPBS, resuspended in DMEM (Corning, 10-013), and kept at 4°C briefly before use the same day.

In vitro hair follicle reconstitution assay

$2x10^6$ neonatal foreskin keratinocytes and $3x10^6$ fetal scalp dermal cells were resuspended in 120 µl of F12:DMEM (1:1) medium (Gibco Ham's F-12 Nutrient Mix, ThermoFisher; DMEM, Corning) with 5% FBS and P/S/A for a final volume of 140 µl and plated as a droplet on a 6-well cell culture insert set into a matching 6-well plate (Falcon). 1.8 ml of 1:1 medium was added to the well. The droplets were incubated at 37°C and 5% CO_2 for 4-7 days. Growth factors were added to the culture droplet at the following concentrations daily: 1 µg/ml and 10 µg/ml sonic hedgehog (Shh, recombinant human, Peprotech), 0.5 µg/ml transforming growth factor beta 2 (Tgfβ2, recombinant human, Millipore), 1 µM retinoic acid receptor (RAR) antagonist ER 50891 (R&D Systems), 1 µg/ml fibroblast growth factors (FGF) 2, 7, and 10 (recombinant human, Miltenyi, Life Technologies, R&D Systems, respectively), 1 µg/ml Wnt7a (human recombinant, R&D Systems), 660 nM chelerythrine chloride and 10 nM bisindolylmaleimide I protein kinase inhibitors (PKCi, Millipore), 1 µg/ml and 10 µg/ml Noggin (human recombinant, Peprotech),

10 µg/ml Dkk1 (human recombinant, R&D Systems). 4% PFA or 100% methanol was added directly to the cell insert and well to fix the droplet cultures overnight at 4°C for immunostaining.

Patch assay

$2x10^6$ neonatal foreskin keratinocytes and $3x10^6$ fetal scalp dermal cells were resuspended in 50 µl F12:DMEM (1:1) with 5% FBS and injected subcutaneously into the deep dermis of 6-12 week old hairless nude mice (NU/NU, Charles River). The nude mice were housed under standard conditions and were sacrificed for biopsy at 8 weeks post-injection. This protocol complied with ethical regulations regarding animal experimentation and was approved by the University of Southern California IACUC committee.

Immunostaining

Immunostaining was performed on fixed droplet cultures as whole mount specimens or paraffin-embedded sections. Antibodies are listed in Table S1. Images were taken with Zeiss LSM 510meta and 780 confocal microscopes.

Lentiviral vectors

The following vector genome plasmids were cloned from the stock plasmid pCCL-MU3-IRES-eGFP (courtesy of Paula Cannon, USC): pCCL-EF1α-GAP-eGFP, pCCL-K14-H2B-mOrange2, pCCL-MU3-H2B-mOrange2, pCCL-MU3-H2B-mCerulean3, and pCCL-p63-H2B-eGFP. Promoters and fluorescent proteins were amplified from human genomic DNA or plasmids purchased from Addgene. Primers are listed in Table S2.

293T cells at 50-60% confluency were transfected with 10 µg vector genome plasmid, 10 µg of packaging construct ΔR8.2 (P. Cannon, USC), and 2 µg envelope plasmid pCMV-VSVG (P. Cannon, USC) using the calcium phosphate method.[51] 10mM sodium butyrate was added to fresh media 16 hours post-transfection and removed after 8 hours. Virus-containing media was collected at 36 hours post-transfection, sterile filtered, and ultracentrifuged on a 20% sucrose cushion at 25,000 rpm and 4°C for 1.5 hours before storing at -20°C for up to 30 days or -70°C indefinitely.

Human neonatal foreskin keratinocytes were transduced with lentiviral vector, which was removed 4-8 hours later. The foreskin keratinocytes were cultured for at least 2 weeks before fluorescence could be strongly visualized. 10 µl virus was added directly to the *in vitro* hair reconstitution assay droplet at the time of plating for transduction of dermal cells.

Live cell imaging

Live cell confocal imaging was performed after 72 hours of culture. The cell culture insert membrane, including the culture droplet with transduced cells, was removed from the insert frame, suspended between silicone columns, and held in place with magnets inside a 6-cm glass-bottom cell culture dish (Electron Microscopy Sciences, 70674-52) modified with a glass coverslip inserted into the lid to place the cells at the appropriate focal distance for confocal or two-photon imaging. The entire volume of the culture dish was filled with hair follicle reconstitution assay medium and the dish was sealed with silicone caulk to maintain a lentivirus-free outer surface. The culture was imaged on a Zeiss LSM 5 Pascal microscope with a heated stage set to 37°C. A z-stack image was collected every 10 minutes.

Software analysis

Confocal images were processed with ImageJ software. Z-stack confocal images and live cell imaging z-stack series were converted into videos using Bitplane's Imaris software.

Statistical analysis

The statistical significance of differences in means was calculated using a two-sample T-test. Variance was calculated using the F-test. A p-value of <0.05 was considered significant. All error bars represent standard error of the mean. All experiments were performed in triplicate, at a minimum.

Mathematical modeling

We use the following reaction-diffusion model to simulate the interactions of two, as yet, experimentally unidentified, different morphogen populations, denoted u and v. Because of their roles in the equations u is termed the activator (existence of u promotes the production of more u and v) and v is termed the inhibitor (existence of v causes a reduction in the production of u). In turn, the cells read the local concentrations of the activator and inhibitor and determine their fate accordingly. The simulations take place on a circular two-dimensional domain of radius 10, centred at the orgin. We define the standard polar distance from the origin, r, in terms of the Cartesian coordinates (x,y) as $r = \sqrt{x^2 + y^2}$. The equations are, thus,

$$\frac{\partial u}{\partial t} = D_u \nabla^2 u + P_u \frac{u^2}{u^2 + k_1^2} \frac{1}{1 + G(r,t)v} - u,$$

$$\frac{\partial v}{\partial t} = D_v \nabla^2 v + P_v \frac{u^2}{u^2 + k_2^2} + s_v - v,$$

$$\frac{\partial u}{\partial n} = 0 = \frac{\partial v}{\partial n} \quad \text{on the boundary,}$$

$$G(r,t) = \begin{cases} \alpha + r\beta t, & 0 \le t < t_f, \\ \alpha + r\beta t_f, & t \ge t_f. \end{cases}$$

In addition to the standard reaction-diffusion framework we have included a linear spatiotemporal gradient G. The gradient is radially symmetric; it starts flat at time zero and slowly increases at the boundary over time. At time t_f the gradient reaches its maximum value and freezes allowing the simulation to relax to a final heterogeneous steady state. This gradient modulates the inhibitor effect of the morphogen v on u, maximising its effect on the boundary.

Additional parameter values are given in Table S3. All unit dimensions are arbitrary, but consistent. The initial conditions for all populations were uniform random numbers with mean set to the largest positive uniform steady state when $t = 0$, and, hence, $G = \alpha$. The equations were simulated using a finite element Runge-Kutta method and the domain was discretised into 25970 domain elements. Note that the boundary conditions are specified to be zero-flux conditions, meaning that no substances are able to leak out of the domain. Initially, the time step was 10^{-3}, which was decreased as required to satisfy a relative step error tolerance of 10^{-6}. After a simulation was completed the simulation was repeated with double the initial domain elements and half the time step to guarantee convergence, through observing that the result did not change.

Supplemental Figures, Movies, and Tables

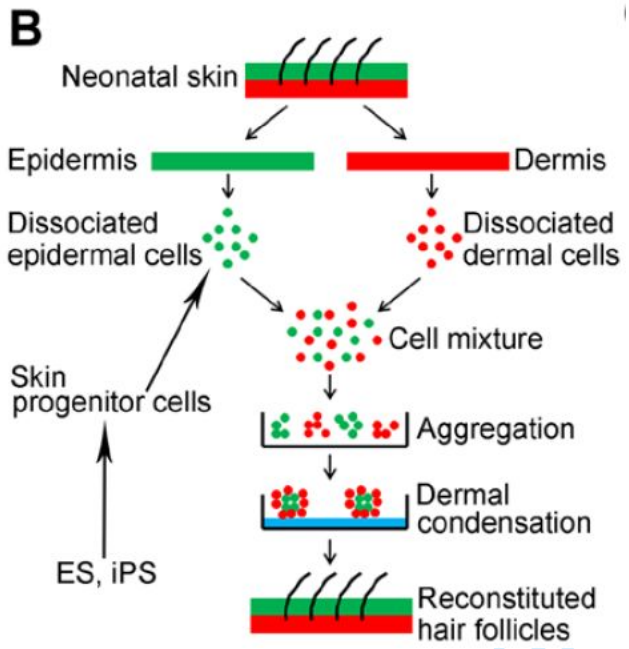

Figure S1. A generic working model for planar skin reconstitution with hair formation. Epidermal and dermal cells are mixed and plated on tissue culture insert in high cell density as a droplet. Different epidermal and dermal cells can be used, those derive from newborn skin, adult skin, adult hair follicle, and ES or iPS derived cells.

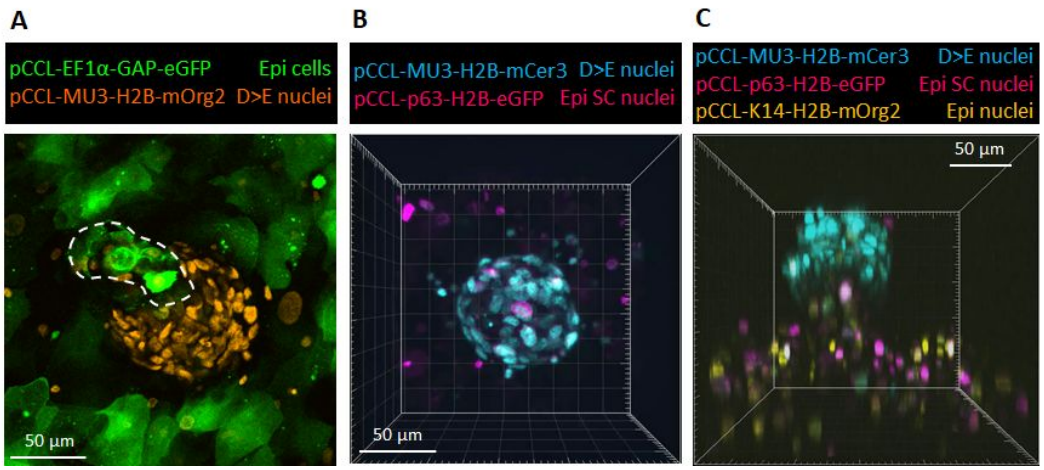

Figure S2. Live cell imaging of hair peg-like structures.

A. Overexpression of fluorescent proteins did not affect the ability to form hair peg-like structures. In this image, epidermal cell nuclei were marked with green fluorescent protein and dermal cell nuclei were preferentially marked with orange fluorescent protein. The dotted line outlines the epidermal stalk. Epi = epidermal, D = dermal, E = epidermal. (n=7)

B. A still image from a two-color live imaging video (Fig. S5A), looking down from the top of the culture droplet, demonstrates a dermal cap. p63-positive keratinocyte nuclei are magenta, dermal cell nuclei are cyan. Epi SC = epidermal stem cell. (n=5)

C. A single lateral image taken from a three-color live imaging video (Fig. S5B) demonstrates a hair peg-like structure. Keratinocyte nuclei are orange, p63-positive keratinocyte nuclei are magenta, and dermal cell nuclei are cyan. (n=5)

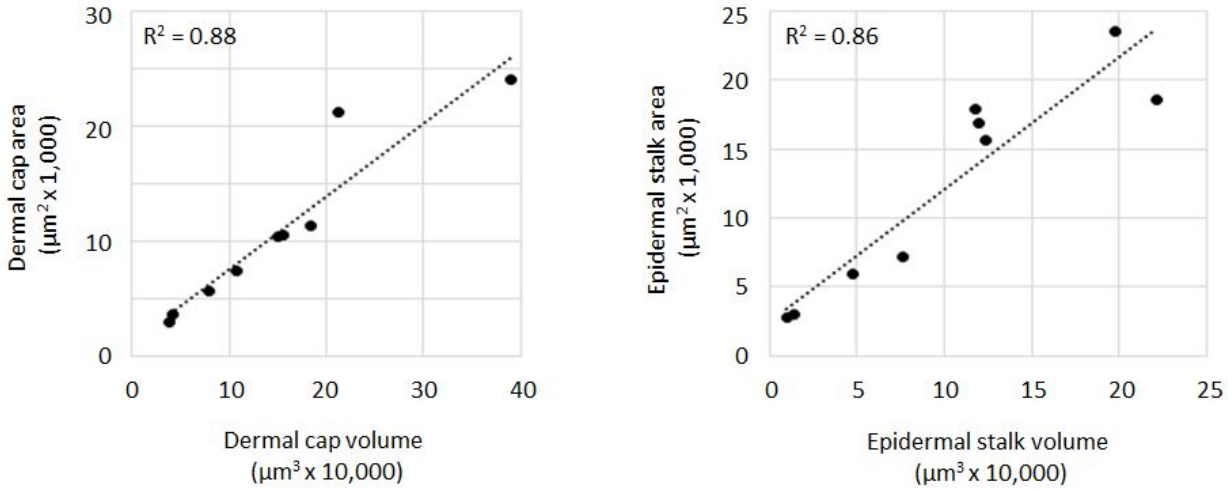

Figure S3. Reconstituted hair peg-like structures displayed radial symmetry.

Cap and stalk sagittal areas maintained a linear relationship with the total cap and stalk volumes, emphasizing the radial symmetry of these structures and allowing us to simplify analysis by measuring the area of each structure at the midpoint corresponding to maximal width.

Movie S1. Three-dimensional z-stack reconstructions of human hair peg-like structures formed in culture.

A. Whole mount confocal z-stack images of multiple hair peg-like structures immunostained with keratin-14 (green), vimentin (red), and TO-PRO-3 iodide (nuclei, blue) demonstrate the periodic patterning and formation of distinct structures within a 425 μm^2 area. Cells within the keratinized sheet were difficult to stain with pancytokeratin due to poor antibody penetration.

B. Whole mount confocal z-stack images of hair peg-like structures immunostained with pancytokeratin (green) and propidium iodide (nuclei, red) demonstrate the spherical configuration of the dermal cap and the tubular structure of the epidermal stalk. Sandwiching of the whole mount culture beneath a coverslip for confocal imaging caused the hair pegs to appear bent or flattened against the keratinocyte sheet.

C. Higher magnification view of a single reconstituted human hair peg-like structure immunostained with pancytokeratin (green) and propidium iodide (nuclei, red). Note epidermal cells start to wrap around the dermal cap.

Movie S2. Three-dimensional z-stack reconstructions of reconstituted human hair peg-like structures demonstrate markers of dermal papilla gene expression.

A. Whole mount confocal z-stack imaging demonstrates α-SMA staining in a central location within the dermal cap of a hair peg-like structure. α-SMA (green), propidium iodide (red).

B. Whole mount confocal z-stack imaging demonstrates the presence of extracellular collagen IV at the epidermal-dermal interface. CD34 - an early dermal papilla marker (green), collagen IV (red), TO-PRO-3 iodide (blue). The large green lobules are artifacts representing dead cells which have trapped the dye.

Movie S3. Three-dimensional z-stack reconstructions of epidermal placode-like structures and dermal clusters at 48 hours.

A. Whole mount confocal z-stack imaging demonstrates multiple dermal clusters atop a keratinocyte sheet and altered keratinocyte arrangement pattern around the dermal clusters. Pancytokeratin (green), propidium iodide (red). The large green lobules are artifacts representing dead cells which have trapped the dye.

B. Whole mount confocal z-stack imaging demonstrating vimentin-positive immunostaining of the dermal clusters at 48 hours post-plating. Vimentin (red), TO-PRO-3 iodide (blue).

Movie S4. Live cell imaging of a reconstituted human hair peg-like structure.

Time-lapse movie highlighting dermal cell shape and movement within the dermal cap of a reconstituted human hair peg-like structure, as viewed from the top of a culture droplet. The epidermal stalk is not visible in this view. A z-stack image was recorded every 10 minutes from 101-103 hours post-plating and is replayed at a rate of 5 frames per second. The entire culture descended along the z-axis during imaging, resulting in partial movement out of the focal plane over time. p63-positive epidermal cells were labelled with nuclear eGFP fluorescent protein (magenta). Dermal cells were labelled with nuclear mCerulean3 fluorescent protein (cyan). Note the varied dermal cell movement and nuclear shape within the dermal cap. Few p63-positive epidermal cells are visible in this top-down view, as the epidermal stalk is obscured by the cells of the dermal cap. However, reproducibly, 1-3 p63-positive epidermal cells were noted within the dermal cap, frequently at the apex, as seen here.

Movie S5. Live cell imaging of a reconstituted human hair peg-like structure.

Time-lapse movie of a reconstituted human hair peg-like structure, viewed from top-down (**A**) and lateral (**B**) orientations. A z-stack image was recorded every 10 minutes from 83-85 hours post-plating and is replayed at a rate of 10 frames per second. All epidermal nuclei were pre-labelled with mOrange2 fluorescent protein (yellow). p63-positive epidermal nuclei were labelled with eGFP (magenta). Dermal nuclei were labelled with mCerulean3 fluorescent protein (cyan). Note that the entire specimen drifts during imaging. However, the epidermal cells within the epidermal sheet remain static, as evidenced by no change in positional relationship with adjacent epidermal cells. The position of the dermal cap does move in space, relative to the epidermal sheet, because the epidermal stalk is flexible and sways within the droplet culture medium.

Movie S6. Mathematical simulation of human hair follicle periodic pattern formation *in vitro*.

The changes in periodic patterning from long stripes to short stripes to punctate clusters, corresponding to dermal clusters and then hair peg-like structures, is represented here by a Turing-based mathematical simulation. The periodic patterns form sequentially on the left, as the radially symmetric spatiotemporal gradient increases in the middle and right-sided diagrams.

Table S1. Antibodies.

Antibody	Source	Catalog Number	Dilution
Alkaline phosphatase	Abcam	ab108337	1:100
α-SMA	ThermoFisher	MA1-37028	undiluted
β-catenin	Sigma	C7207	1:100
CD34	Millipore	CBL496	1:100
Collagen I	Abcam	ab34710	1:100
Collagen III	Abcam	ab7778	1:100
Collagen IV	Abcam	ab19808	1:100
Cytokeratin 14/15/16/19 (pancytokeratin)	Becton Dickinson	550951	1:100
Keratin-10	ThermoFisher	MA5-11599	1:100
Keratin-14	ThermoFisher	MS-115-P1	1:100
Laminin 5	Abcam	ab14509	1:100
p63	Santa Cruz	Sc-8343	1:100
PCNA	Abcam	ab92552	1:100
Propidium iodide	Sigma	P4170	1:1000
TO-PRO-3 iodide	ThermoFisher	T3605	1:500
Vimentin	Cell Signaling	3390	1:100

Table S2. Primers for lentiviral vector construction
gDNA = genomic DNA

Sequence	Forward primer	Reverse primer	Amplified from	Source
EF1α promoter	ATAAATGAATTCGCTCCGGTGCCCGTCAG	GCCCAGGAATTCTCACGACACCTGAAATGG	plasmid RBW1	Chuong lab
p63 promoter	TTCGGGGCTAGCGTAAGTAGGTTTTTTTTT	TAAGCTGCTAGCGTTAGCTGTAAGATTGATC	Human gDNA	293T cells
K14 promoter	TTATATGAATTCCCCGGGCTCCGGAGCTTC	GCTGGGGAATTCCTCGGGTAAATTGGAAAG	Human gDNA	293T cells
H2B-mOrange2	TAGATTGCTAGCATGCCTGAACCC	TAAGATGCTAGCTCACTTGTACAGC	plasmid #57962	Addgene
GAP-eGFP	TAGATTGGATCCATGCTGTGCTGTATG	TAAGATGGATCCTTACTTGTACAGCTCG	plasmid #14757	Addgene
H2B-eGFP	TAAAATGCTAGCATGCCTGAGCCGGCCAAG	GCCCGAGCTAGCTTACTTGTACAGCTCGTC	RCAS-H2B-eGFP	Chuong lab
H2B-mCerulean3	TTTATTGCTAGCATGCCAGAGCCAGCGAAG	GGGTAGGCTAGCTTACTTGTACAGCTCGTC	plasmid #55374	Addgene

Table S3. Parameter values for equations (1)-(4).

Parameter	Value	Definition
P_u	1000	Strength of influence of activator on activator
P_v	100	Strength of influence of activator on inhibitor
k_1	10	Activator sensitivity to activator
k_2	10	Inhibitor sensitivity to activator
s_v	1	Inhibitor source
D_u	2.5×10^{-4}	Activator diffusion rate
D_v	1.25×10^{-2}	Inhibitor diffusion rate
α	1.1	Basal level of gradient
β	1/250	Rate of gradient increase
t_f	150	Time after which the gradient stops evolving

USC
UNIVERSITY OF SOUTHERN CALIFORNIA

Keck School of Medicine
University of Southern California

Department of Pathology and Laboratory Medicine

Laboratory of Tissue Development and Engineering

Cheng-Ming Chuong, M.D., Ph.D.
Professor and
Laboratory Director
Tel: 323 442-1296
email: cmchuong@usc.edu

Faculty:

Randall B. Widelitz, Ph.D.
Tel: 323 442-1158
email: widelitz@usc.edu

Ting-Xin Jiang, M.D.
Tel: 323 442-1158
email: tjiang@usc.edu

Ping Wu, Ph.D.
Tel: 323 442-1982
Email: pingwu@usc.edu

Laboratory Website
http://www-hsc.usc.edu/~cmchuong

2011 Zonal Avenue
Hoffman Medical
Research Building 313
Los Angeles,
California 90089-9092
Fax: 323 442-3049
webpage: http://www.usc.edu/medicine/pathology

October 12th, 2018

Dear editor:

We are submitting the manuscript, entitled "Self-organizing hair peg-like structures from dissociated skin progenitor cells: New insights for human hair follicle organoid engineering and Turing patterning in an asymmetric morphogenetic field," for publication as a research article in *Experimental Dermatology*.

The quest to tissue engineer organs is at the forefront of translational research today. Patients suffering from burns and those with alopecia would benefit greatly from the ability to tissue engineer replacement hair follicles. While much work has been done in the mouse, human hair follicle regeneration has proven much more difficult. We have developed an *in vitro* culture system, which supports the rapid regeneration of human hair peg organoids from human epidermal and dermal skin progenitor cells. This culture system is easily perturbed and affords the unique opportunity to analyze self-assembly behavior in detail and modulate physical and chemical parameters to more effectively stimulate follicular regeneration. Furthermore, the model presents a great opportunity to study Turing patterning in an asymmetric morphogenetic field. We take a multi-disciplinary approach and develop a mathematical model to simulate and predict this type of behavior.

We made progress in developing a useful new platform for identifying molecules involved in human hair tissue engineering, in collective cell behavior during self-assembly of human hair primordia, and in progressive patterning of hair primordium population. The significance of this study would be of general interest to the readership of *Experimental Dermatology*. We have prepared this manuscript for the special issue on skin morphogenesis edited by Plikus and Chuong.

Because of the complexity of the work, currently we have 4752 words. I hope you can allow some flexibility of the word limit.

This manuscript describes original work and is not under consideration of any other journal. We look forward to hearing your response. Thank you

Sincerely,

Cheng-Ming Chuong
Department of Pathology
University of Southern California
Keck School of Medicine
2011 Zonal Ave., HMR 313B
Los Angeles, CA 90033

a) Category: Regular Article

b) This article is a solicited submission. For the special issue on skin morphogenesis edited by Plikus / Chuong.

c) The guidelines for a regular article have been fully respected.

d) The quest to tissue engineer organs is at the forefront of translational research today. Patients suffering from burns and those with alopecia would benefit greatly from the ability to tissue engineer replacement hair follicles. While much work has been done in the mouse, human hair follicle regeneration has proven much more difficult. We have developed an *in vitro* culture system, which supports the rapid regeneration of human hair peg organoids from human epidermal and dermal skin progenitor cells. This culture system is easily perturbed and affords the unique opportunity to analyze self-assembly behavior in detail and modulate physical and chemical parameters to more effectively stimulate follicular regeneration. Furthermore, the model presents a great opportunity to study Turing patterning in an asymmetric morphogenetic field. We take a multi-disciplinary approach and develop a mathematical model to simulate and predict this type of behavior.

e) Keywords: Skin reconstitution, tissue engineering, hair follicle, periodic pattern formation, organogenesis

f) Recommended reviewers:

Tissue engineering:
Steven Boyce
University of Cincinnati
steven.boyce@uc.edu
Expert in engineered skin substitutes and regenerative medicine

Pattern:
Philip Murray
University of Dundee
pmurray@maths.dundee.ac.uk
Expert in hair follicle growth patterning and modeling

g) None of the suggested referees has co-authored a publication during the past 4 years with any of the co-authors of the submitted manuscript.

USC
UNIVERSITY OF SOUTHERN CALIFORNIA

Keck School of Medicine
University of Southern California

Department of Pathology and Laboratory Medicine

Laboratory of Tissue Development and Engineering

Cheng-Ming Chuong, M.D., Ph.D.
Professor and
Laboratory Director
Tel: 323 442-1296
email: cmchuong@usc.edu

Faculty:

Randall B. Widelitz, Ph.D.
Tel: 323 442-1158
email: widelitz@usc.edu

Ting-Xin Jiang, M.D.
Tel: 323 442-1158
email: tjiang@usc.edu

Ping Wu, Ph.D.
Tel: 323 442-1982
Email: pingwu@usc.edu

Laboratory Website
http://www-hsc.usc.edu/~cmchuong

2011 Zonal Avenue
Hoffman Medical
Research Building 313
Los Angeles,
California 90089-9092
Fax: 323 442-3049
webpage: http://www.usc.edu/medicine/pathology

December 20th, 2018

Subject: Revision and resubmission of manuscript EXD-18-0381

Dear editors:

Thank you for your letter enclosing the reviewers' comments and the opportunity to revise our manuscript entitled "Self-organizing hair peg-like structures from dissociated skin progenitor cells: New insights for human hair follicle organoid engineering and Turing patterning in an asymmetric morphogenetic field." We appreciate the insightful comments and the suggestions from you and the reviewers.

We have carefully reviewed the comments, and responded to them **point-by-point**. As suggested, we also updated the discussion with recent papers. The reviews have been very helpful and the manuscript has improved. The length is a little bit over the limit, but I have communicated with Dr. Paus for the permission to have some flexibility. The revisions in the text are marked in yellow as requested.

The revision has been approved by all authors. We hope the revised manuscript is now acceptable for *Experimental Dermatology* but are happy to consider further revisions as needed. We thank you for your support.

Thank you.

Sincerely,

Cheng-Ming Chuong
Department of Pathology
University of Southern California
Keck School of Medicine
2011 Zonal Ave., HMR 313B
Los Angeles, CA 90033

Reviewer Comments, Author Responses and Manuscript Changes

Reviewer 1

Weber et al. present a study of hair follicle (HF) formation in vitro via organoids, with an accompanying mathematical model. This study advances our understanding of de novo HF generation in vitro, and may help future protocols by describing parameters and model dynamics that help drive this process. The Turing-based model that is developed is interesting from a theoretical perspective, and produces qualitative behavior that mirrors the experimental system. Given the culture system, which seeks to understand (and grow) HFs resulting from interactions between dermal and epidermal cells, I think a model that contained at least a hint of dermal/epidermal ingredients and molecular detail may be more relevant, however I realize this is probably outside of the current scope. Below I list some questions that are either requests for clarification or suggestions that I think would help to strengthen the manuscript.

Comment 1: "…to ones where the "reactants" are cells themselves to mechanochemical models which couple cell interactions with chemical signals." - please cite examples.

Response: Several papers which discuss mechano-chemical coupling in the generation of biological patterns are listed below [1-5].

1. Oster, G.F., J.D. Murray, and A.K. Harris, *Mechanical aspects of mesenchymal morphogenesis.* J Embryol Exp Morphol, 1983. **78**: p. 83-125.
2. Kondo, S. and T. Miura, *Reaction-diffusion model as a framework for understanding biological pattern formation.* Science, 2010. **329**(5999): p. 1616-20.
3. Nakamasu, A., et al., *Interactions between zebrafish pigment cells responsible for the generation of Turing patterns.* Proc Natl Acad Sci U S A, 2009. **106**(21): p. 8429-34.
4. Murray, J.D., P.K. Maini, and R.T. Tranquillo, *Mechanochemical models for generating biological pattern and form in development.* Physics Reports, 1988. **171**(2): p. 59-84.
5. Ho, W.K.W., et al., *Feather Arrays are Patterned by Interacting Signalling and Cell Density Waves.* PLoS Biol, in press.

These references are now added and discussed in the text.

Comment 2: "This change of topology results from powerful interactions between dermal condensations like dermal cap cells and epidermal progenitors in the basal layer." What mediates these?

Response: We hypothesize that the process is dependent on epithelial-mesenchymal interactions. We have not identified the molecular mediators and have deleted this aforementioned sentence.

Comment 3: Fig. 3D - I don't know if it is appropriate to compare the number of hair pegs at different radii (and then do a t-test). In polar coordinates, wouldn't this introduce artifacts? Instead can you use the density of hair pegs?

Response: We have recalculated using the density of hair pegs in each zone. The figure, figure legend, and text were updated accordingly.

Comment 4: "Centrally, dermal aggregates were 60% larger in diameter, which correlated with the formation of less mature hair peg-like structures and, in many cases, abnormal aggregates possessing multiple epidermal stalks" - do you think this also results from the geometry of the system?

Response: Yes, we believe this is an effect of the physical culture system. For example, we observed differences in the number of hair peg-like structures and abnormal-appearing aggregates when epidermal:dermal cell ratios

were altered. Based on gross observations, the distribution and density of epidermal and dermal cells varied throughout the volume of the droplet. Thus, the droplet environment, which includes cell ratios, mechanical forces, and/or chemical media (which can create a gradient across the radius), is not the same throughout the droplet. In this study, we did not examine whether the formation of hair peg-like structures versus abnormal aggregates is a direct result of the geometry of the droplet shape or the difference in epidermal-dermal cell ratio between the center and periphery. Therefore, we have chosen to use "asymmetric morphogenetic field" in the title.

Comment 5: 'figure "simulation" '— should be Figure 3?

Response: Yes, we added the figure reference to lines 260 and 281.

Comment 6: Regarding the model, I appreciate that, as the authors describe, "…this work is not about specifying the exact underlying kinetics" and that "our results have put an upper bound limit on the complexity required to make a model consistent with the observed results." Nonetheless, after the development of this model, it seems to be sold short. I think that even a little model analysis would be of great interest to the reader, significantly enhance the applicability of the work, and help to understand how these complex patterns emerge. E.g. Model/parameter sensitivity, esp. regarding Turing parameters vs. gradient parameters? Perturbations? E.g. how readily can the dot—labyrinth pattern be changed? Can the wave speed be regulated by Turing parameters rather than solely the gradient? Any predictions here could be added to — and benefit — the section on "A platform to modulate hair peg morphogenesis in vitro." I think that only with some of these additions can you really say that you "predict conditions that may enhance organoid formation."

Response: Two-dimensional Turing patterns can produce spots and/or stripes, depending on the ratio of the sum of activator activities / sum of inhibitor activities. When the morphogenetic field is even, all elements, whether they are supposed to be spots or stripes, may occur simultaneously. When the field is asymmetrical, they may occur in sequence, with elements emerging when conditions are met [6]. Thus, as long as the correct pattern kinetics are chosen to produce in phase, or out of phase, patterns between the concentrations, the Turing system can be guided to form spots and/stripes. Further, a parameter's influence is extremely local in Turing patterns [7]. Thus, all we require to convert a system from spots to stripes is to use a gradient that influences the competition between the cubic and quadratic terms. Depending on the level of activator and inhibitor and types of cells (with different response threshold to activators and inhibitors), the droplet can exhibit a range of stripe to spot morphology. This is a generic and robust mechanism. As such, we do not feel that a sensitivity analysis is essential, as this would depend on the kinetics chosen, which (as stated) are ad-hoc, arbitrary and inconsequential.

For the "wave", a timely paper by the Headon group reporting a global wave has recently been accepted in PLOS Biology [5]. Our lab also wrote a primer (**Turing patterning with and without a global wave)** for it [8]. The following paragraph has been added to the discussion, on lines 420-430.

"In vivo, chicken feather buds form exquisite hexagonal patterns progressively from the midline to the flank. Earlier works have suggested this results from a local Turing event and a global propagating events (Jiang et al., 1999). However, the nature of the global even is unknown. This is part of the motivation for this study, to use the organoid droplet to understand more about the nature of the sequential appearance of hair or feather primordia. It is timely that a paper reporting a global Eda wave spreading from the midline to the flank is just reported, which suggests Eda induces FGF20, followed by dermal cell aggregate formation, thus facilitating Turing patterning via mechano-chemical coupling (Ho et al., in press). Based on this and other studies, we propose a new integrated understanding that a Turing periodic patterning occurs with or without a global propagation mechanism. The global mechanism can be chemical or mechanical in nature, as long as they can tilt Turing activator / inhibitor system (Inaba et al., in press). The asymmetric morphogenetic field in the organoid culture studied here presents a good model to further test how this global asymmetry mechanism works. "

By separating the patterning mechanism into local Turing mechanism and global influence (due to the asymmetric morphogenetic field), the issues are much clearer now. In terms of the wave speed, the dynamics can be translated to how fast the global wave travels or how steep the chemical or physical gradients are. We have added text regarding the robustness, generality and interpretation of the mechanism. The following references have been cited.

5. Ho, W.K.W., et al., *Feather Arrays are Patterned by Interacting Signalling and Cell Density Waves.* PLoS Biol, in press.
6. Ermentrout, B., *Stripes or spots? Nonlinear effects in bifurcation of reaction—diffusion equations on the square.* Proceedings of the Royal Society of London. Series A: Mathematical and Physical Sciences, 1991. **434**(1891): p. 413-417.
7. Krause, A.L., et al., *Heterogeneity induces spatiotemporal oscillations in reaction-diffusion systems.* 2018. **97**(5): p. 052206.
8. Inaba, M., H.I.-C. Harn, and C.M. Chuong, *Turing patterning with and without a global wave.* PLoS Biol, in press.

Comment 7: Model development: "existence of v causes a reduction in the production of u and v" — there is no term in the equation for dv that describes self-inhibition. Please clarify.

Response: Thank you for pointing out this typo in supplemental information line 123: Existence of v causes a reduction in the production of u and v --> changed to existence of v causes a reduction in the production of u.

Comment 8: Fig. S2 and Movie S5A,B: looks like stratification has not occurred between precursor and mature keratinocyte? Does this occur later?

Response: Figure S2C and movies S5A,B were taken between 80 and 90 hours of culture. Stratification has occurred at this point, as not all keratinocytes are p63 positive (magenta color). Lentiviral transformation efficiency approached 100% so we can presume that those keratinocytes which are no longer p63+ have differentiated from the epidermal precursor state. In our system, we do see that a high proportion of the epidermal sheet expresses K14, which is a deviation from endogenous epidermis. However, we do also see a layer of cells which expresses K10 and a layer which is positive for involucrin, both of which are not assessed in these videos / still images. To achieve live imaging, the cell culture inserts with the droplets are removed from the insert ring, submerged completely in media, suspended between columns, and held in place with magnets. Thus, the inserts move slightly within the cell culture medium, and it is difficult to obtain, in cross-section, a precise orthogonal view of the culture insert and droplet. The view in Movie S5B is likely a composite view of multiple levels of the epidermal sheet in cross-section, due to the non-rigid nature of the insert. The view in Movie S5A is looking from the top of the droplet down onto the insert and, thus, it is difficult to assess the linear stratification of the epidermal sheet from that perspective.

Comment 9: Typo/word missing? "For human cells, the stages of morphological transition of in this culture system"

Response: Corrected. Thank you.

Reviewer 2

This manuscript seeks to assign a 'Turing model' to observations of cell clustering in vitro, which make 'hair follicles'. As an intriguing cell culture phenomenon this is an interesting paper, however the results fail to convince me that follicles are being made via a Turing patterning. I have therefore separated my comments into those related to the hair follicle, and those related to the model for clarity.

Comment 1: ***Hair follicle***
The hair follicles in 1E look convincing but my concern is they are pigmented…why is this the case if only keratinocytes and fetal dermal cells were co-cultured? Were melanocytes in the mix as well?

Response: While melanocytes were not specifically added as part of the co-culture, there are two possible ways that pigmented cells may have been incorporated. 1) The human keratinocytes were isolated from neonatal foreskins from patients of multiple ethnicities. Once isolated, the keratinocytes were cultured for several passages before use, to amplify sufficient quantities. It is possible that some melanocytes were carried over, though keratinocyte cultures appeared uniform. Cell sorting was not performed to ensure a pure population of keratinocytes. 2) Some fetal scalp specimens contained early hair follicles with slight pigmentation at the base (matrix cells). The epidermis and hair shafts were manually removed from the fetal scalp specimens, leaving the dermal portion for use, but it is possible that some pigmented progenitor cells remained associated with the dermal papilla / dermal sheath. The dermal cells were not cultured or sorted and so these pigmented cells may have been included. The neonatal keratinocytes and fetal dermal cells were injected subcutaneously into nude mice, whose hair follicles do not contain pigment and whose melanocytes do not produce significant melanin. Thus, it is less likely that the pigmentation is derived from murine melanocytes.

Comment 2: ***Hair follicle***
In figure 2 the authors use a wide range of markers to show 'hair identity', yet in my opinion none of the markers they use are actually hair specific-they are all just dermal or epidermal specific. To show that hair follicles have actually formed rather than self organised clusters of cells one would have to show specific dermal papilla (eg syndecan, sox2) and epithelial germ markers (eg p-cadherin). Bizarrely, the only dermal papilla markers used (alk phos) was shown to be expressed in 17wk scalp but not in the cultured hair follicles.

Response: Additional immunostained images were added to Figure 2, demonstrating syndecan and versican positivity of the dermal cap, two frequently used markers of the dermal papilla. It should be noted that we do not claim that the structures formed are mature hair follicles, nor are the dermal caps mature dermal papillae, as we have called the structures hair peg-like. We point out that the dermal cap is likely an immature or incomplete dermal papilla, as it expresses some of the well-known proteins commonly associated with the dermal papilla but not others (ex. alkaline phosphatase). The only definitive way to prove that the dermal cluster is a mature dermal papilla is to show inductivity, which would require mechanical excision of the dermal cap from the peg-like structures and application to numerous murine hair-forming assays. Rather, the goal of this study was to evaluate the ability of dermal fetal scalp populations to self-organize and direct the formation of follicular organoids rapidly in culture, with the future goal of clinically-relevant tissue regeneration.

One must acknowledge that the current literature largely reflects "markers" of the adult, cycling murine hair follicle and dermal papilla and that many "markers" of the dermal papilla, for example, are present only during specific stages within the hair cycle. Much less is known about the human hair follicle, and extremely little has been published on specific human follicle and papilla markers during fetal development. Because there are already known discrepancies between mouse and human follicle staining patterns and architectural organization (ex. epidermal bulge), we tested several of the more commonly used murine markers on human fetal scalp skin. We discussed the challenges with alkaline phosphatase and α-SMA staining. We have added syndecan and versican immunostaining results. In our hands, the murine/human markers CD133 and CD10 were not positive on intact fetal scalp. We did not test Sox2, as it has not been documented to play a role in the human dermal papilla. B-catenin and CD34 are documented markers of the early dermal condensate and we have shown those results. Of course, all of the documented "markers" of the hair follicle or dermal papilla are proteins which are not specific to the hair follicle or the dermal papilla. We have chosen to highlight the similarities of our hair peg-like structures to normal follicular development, using multiple antibodies, and fully acknowledge that these structures are not mature follicles. However, these peg-like structures were reproducible and we believe that, at least, self-assembly or early development into hair peg-like structures has consistently occurred.

Figure 2 has also been updated to include additional epidermal staining, with K17, K18, and E-cadherin antibodies. Very little is known about the expression patterns of the epidermal portion of a hair germ or peg. We do know that, during later stages of development, the epidermal portion stratifies into multiple layers, including the inner and outer root sheaths, which then selectively express K17, K18, or E-cadherin, among other classic marker proteins. However, at the hair peg stage, the epidermal stalk is a solid tube of cells and has not yet stratified into layers surrounding a lumen with hair shaft. Thus, it is difficult to really prove the targeted and appropriate staining of our hair peg-like epidermal stalks. Schirren, et al., studied keratin expression patterns in fetal scalp follicles and demonstrated that the germ is positive for K17. We also acknowledge that K17 is frequently upregulated in wound healing and could solely represent changes in expression induced by epidermal/dermal disruption and culture. For this reason, we were hesitant to include the K17 results at first. Notably, we did test p-cadherin antibodies and found that our structures were p-cadherin negative.

We have also added a few new images of larger, seemingly more mature peg-like structures that we occasionally noted, which appeared to have a more organized epidermal stalk and, possibly, an effort toward the formation of a lumen. We acknowledge that the organoid structures are not real hair follicles and, in fact, call them" hair peg-like structures" in the title. However, we have made progress which we think is worthy of report. In the future, we hope to achieve more mature follicle-like structures *in vitro* under the right conditions.

Comment 3: *Model*

The model description is a bit contradictory. Initially, the authors write that stripes appear, then gradually become rounded into clusters. This would be characteristic of a reaction diffusion model, which can produce spatiotemporal gradients. However, the authors then write that their patterns occur simultaneously, which contradicts their earlier statement. They use this to justify that a spatiotemporal gradient must be present.

Response: Thank you for the opportunity to clarify. We do not mean "their patterns occur simultaneously". Indeed, this paper is meant to say when Turing patterning occurs on an asymmetric field, periodic patterning will occur in progression. When activator / inhibitor activity are tilted in the morphogenetic field (such as the droplet here), reaction-diffusion systems can form a spatiotemporal gradient. The asymmetry of the droplet culture helps produce the asymmetrical pattern, through an effect on chemical or physical parameters.

A paper reporting on a global wave and local Turing patterning by the Headon group has recently been accepted to PLOS Biology[5] and our laboratory wrote a primer (**Turing patterning with and without a global wave)** for it[8]. The following paragraph has been added to the discussion, on lines 420-430.

"In vivo, chicken feather buds form exquisite hexagonal patterns progressively from the midline to the flank. Earlier works have suggested this results from a local Turing event and a global propagating events (Jiang et al., 1999). However, the nature of the global even is unknown. This is part of the motivation for this study, to use the organoid droplet to understand more about the nature of the sequential appearance of hair or feather primordia. It is timely that a paper reporting a global Eda wave spreading from the midline to the flank is just reported, which suggests Eda induces FGF20, followed by dermal cell aggregate formation, thus facilitating Turing patterning via mechano-chemical coupling (Ho et al., in press). Based on this and other studies, we propose a new integrated understanding that a Turing periodic patterning occurs with or without a global propagation mechanism. The global mechanism can be chemical or mechanical in nature, as long as they can tilt Turing activator / inhibitor system (Inaba et al., in press). The asymmetric morphogenetic field in the organoid culture studied here presents a good model to further test how this global asymmetry mechanism works. "

Comment 4: *Model*

The authors also write that more hair peg structures formed at the periphery of drops, perhaps leading them to look at a gradient in the drop-however they do not account for the area under analysis which is also increasing. Actually, is increases so much so that the outer circle is 9x larger than the central circle. If the authors adjusted their number of hair pegs in each concentric circle relative to the analysed

area, they would find an almost equal number of hair pegs per area under analysis. This could be a problem as perhaps there is not a gradient in the drop after all.

Response: Hair peg distribution within the droplet was re-analyzed as density of hair pegs, to account for the increasing area. The outer ring is 5.5x larger than the innermost circle. A gradient is still observed, with more hair peg-like structures forming at the periphery. The figure, legend, and text were adjusted accordingly.

Comment 5: *Model*
I would have thought that mechanical forces would be most prominent in driving the patterning observed (as the cells are in a small drop) rather than inhibitors or activators within the drop. However, this is not incorporated into the model.

Response: The reviewer is quite right that a mechanical model could also achieve a patterned state. However, a temporal gradient would still be required to achieve the transition between patterns. Equally, the pattern transitions as illustrated in the reaction-diffusion equation are well-studied and understood. We have discussed that the Turing model now is interpreted based on its activator / inhibitor loop and the factor can be either chemical or physical factors. In this study, we did not obtain data to state whether chemical or mechanical parameters are more important.

Comment 6: *General comments*
The introduction indicates that the model is a generic one for looking at various cells, but they only demonstrate its use with one cell type.

Response: We removed the word "generic" from lines 87 and 90.

Comment 7: *General comments*
The discussion is quite long and it is not clear how it is always related to the presented results.

Response: We have consolidated the discussion section, particularly the first two paragraphs, to more clearly acknowledge the results presented in the paper (production of hair peg-like organoids) and recent relevant literature (listed below).

1. Oster, G.F., J.D. Murray, and A.K. Harris, *Mechanical aspects of mesenchymal morphogenesis.* J Embryol Exp Morphol, 1983. **78**: p. 83-125.
2. Kondo, S. and T. Miura, *Reaction-diffusion model as a framework for understanding biological pattern formation.* Science, 2010. **329**(5999): p. 1616-20.
3. Nakamasu, A., et al., *Interactions between zebrafish pigment cells responsible for the generation of Turing patterns.* Proc Natl Acad Sci U S A, 2009. **106**(21): p. 8429-34.
4. Murray, J.D., P.K. Maini, and R.T. Tranquillo, *Mechanochemical models for generating biological pattern and form in development.* Physics Reports, 1988. **171**(2): p. 59-84.
5. Ho, W.K.W., et al., *Feather Arrays are Patterned by Interacting Signalling and Cell Density Waves.* PLoS Biol, in press.
6. Ermentrout, B., *Stripes or spots? Nonlinear effects in bifurcation of reaction—diffusion equations on the square.* Proceedings of the Royal Society of London. Series A: Mathematical and Physical Sciences, 1991. **434**(1891): p. 413-417.
7. Krause, A.L., et al., *Heterogeneity induces spatiotemporal oscillations in reaction-diffusion systems.* 2018. **97**(5): p. 052206.
8. Inaba, M., H.I.-C. Harn, and C.M. Chuong, *Turing patterning with and without a global wave.* PLoS Biol, in press.

PLOS Biology

Turing patterning with and without a global wave

--Manuscript Draft--

Manuscript Number:	
Full Title:	Turing patterning with and without a global wave
Article Type:	Primer
Keywords:	pattern formation, Turing, reaction diffusion, feather, morphogenesis, EDA, mechano-chemical coupling tissue mechanics, propagation, development, stem cells, skin progenitors collective behavior,
Corresponding Author:	Chuong Cheng-Ming usc Los Angeles, UNITED STATES
First Author:	Masafumi Inaba
Order of Authors:	Masafumi Inaba
	Hans I-Chen Harn
	Chuong Cheng-Ming
Abstract:	Periodic patterning represents a fundamental process in tissue morphogenesis. In chicken dorsal skin, feather formation starts from the midline, then the morphogenetic wave propagates bilaterally, leaving a regular hexagonal array of feather germs. Yet, in vitro reconstitution showed feather germs appear simultaneously, leading to the hypothesis that the feather-forming wave results from the coupling of local Turing patterning processes with an unidentified global event. In this issue, Ho et al. (1), showed such a global event in chicken feathers involves a spreading EDA wave and FGF20-cell aggregate-based mechano-chemical coupling. Interestingly, in flightless birds, feather germs form without waves are irregularly positioned.
Suggested Reviewers:	
Opposed Reviewers:	
Additional Information:	
Question	**Response**
Competing Interests You are responsible for recognizing and disclosing on behalf of all authors any competing interest that could be perceived to bias their work, acknowledging all financial support and any other relevant financial or non-financial competing interests.	no

Do any authors of this manuscript have competing interests (as described in the PLOS Policy on Declaration and Evaluation of Competing Interests)? **If yes**, please provide details about any and all competing interests in the box below. Your response should begin with this statement: *I have read the journal's policy and the authors of this manuscript have the following competing interests:* **If no** authors have any competing interests to declare, please enter this statement in the box: "*The authors have declared that no competing interests exist.*" * typeset	
Ethics Statement You must provide an ethics statement if your study involved human participants, specimens or tissue samples, or vertebrate animals, embryos or tissues. It is your responsibility to provide this information, and by completing this question, you confirm responsibility. All information entered here should **also be included in the Methods section** of your manuscript. Please write "N/A" if your study does not require an ethics statement. We encourage authors to comply with the Animal Research: Reporting In Vivo Experiments (ARRIVE) guidelines, developed by the National Centre for the Replacement, Refinement & Reduction of Animals in Research (NC3Rs). If you	N/A

have an ARRIVE checklist, please upload it as an 'Other' item type in the Attach Files section.

Human Subject Research (involved human participants and/or tissue)

All research involving human participants must have been approved by the authors' Institutional Review Board (IRB) or an equivalent committee, and all clinical investigation must have been conducted according to the principles expressed in the Declaration of Helsinki. Informed consent, written or oral, should also have been obtained from the participants. If no consent was given, the reason must be explained (e.g. the data were analyzed anonymously) and reported. The form of consent (written/oral), or reason for lack of consent, should be indicated in the Methods section of your manuscript.

Please enter the name of the IRB or Ethics Committee that approved this study in the space below. Include the approval number and/or a statement indicating approval of this research.

Animal Research (involved vertebrate animals, embryos or tissues)

All animal work must have been conducted according to relevant national and international guidelines. If your study involved non-human primates, you must provide details regarding animal welfare and steps taken to ameliorate suffering; this is in accordance with the recommendations of the Weatherall report, "The use of non-human primates in research." The relevant guidelines followed and the committee that approved the study should be identified in the ethics statement.

If anesthesia, euthanasia or any kind of animal sacrifice is part of the study, please include briefly in your statement which substances and/or methods were applied. Manuscripts describing studies that use death as an endpoint will be subject to additional ethical considerations, and may be rejected if they lack appropriate justification for the study or consideration of humane endpoints.	
Please enter the name of your Institutional Animal Care and Use Committee (IACUC) or other relevant ethics board, and indicate whether they approved this research or granted a formal waiver of ethical approval. Also include an approval number if one was obtained.	
Field Permit If this is a field study, or involves collection of plant, animal, or other materials collected from a natural setting, please provide your field permit number and indicate the institution or relevant grant body that granted permission for use of the land or materials collected.	

Dr. Di Jiang:

Here is the primer " **Turing patterning with and without a global wave".**
Thanks for the invitation.
Finally we are able to submit it.

Best regards

Cheng-Ming Chuong, MD, PhD
鍾正明
Professor of Pathology
Chair, Graduate Committee
Univ. Southern California
2011 Zonal Avenue, HMR 313
Los Angeles, CA 90033
(O) 323 442 1296 (M) 949 413 4942
http://www-hsc.usc.edu/~cmchuong/

Academician, Academia Sinica
中央研究院院士

Turing patterning with and without a global wave

Masafumi Inaba[1], Hans I-Chen Harn[1,2], and Cheng-Ming Chuong[1,2,3]

Author Affiliations:

[1] Department of Pathology, Keck School of Medicine, University of Southern California, Los Angeles, CA, USA
[2] International Research Center of Wound Repair and Regeneration (iWRR), National Cheng Kung University, Tainan, Taiwan
[3] Integrative Stem Cell Center, China Medical University Hospital, China Medical University, Taichung, Taiwan

Funding:

M.I. is supported by Human Frontier Science Program (LT001148/2015-L). HIH is supported by grant from Ministry of Education of Taiwan. CMC is supported by NIH Grants AR47364, AR60306, and GM125322.

Abstract

Periodic patterning represents a fundamental process in tissue morphogenesis. In chicken dorsal skin, feather formation starts from the midline, then the morphogenetic wave propagates bilaterally, leaving a regular hexagonal array of feather germs. Yet, in vitro reconstitution showed feather germs appear simultaneously, leading to the hypothesis that the feather-forming wave results from the coupling of local Turing patterning processes with an unidentified global event. In this issue, Ho et al. [1], showed such a global event in chicken feathers involves a spreading EDA wave and FGF20-cell aggregate-based mechano-chemical coupling. Interestingly, in flightless birds, feather germs form without waves are irregularly positioned.

Regular periodic feather patterns on the chicken skin

Animal integuments exhibit periodic patterns in spots, stripes or mazes, which are made of pigment domains, hairs or feathers. In the developing chicken embryo, one of the most fascinating phenomena is that feather buds begin to form at the dorsal midline around embryonic day 6, then propagate bilaterally toward the flank, leaving a highly ordered array of feather germs arranged in a hexagonal pattern after about three days [2–4].

Is this patterning process a playout of a molecular blueprint (like in Drosophila) or the result of stochastic local interactions? Perturbation experiments leading to altered patterns suggest the system is plastic [5,6] and skin progenitors are not pre-determined to be a bud or an interbud cell. For local interactions, one fundamental theory is based on Turing's reaction-diffusion) model [7,8]. Turing showed hypothetical chemical reactions could form periodic structures spontaneously in a situation where an activator activates its own production and a long-range inhibitor that represses the activator. When the inhibitor diffusion rate is much larger than that of activator, those chemicals are distributed heterogeneously, forming periodic patterns such as spots and stripes (Fig. 1A).

In feathers, FGF and BMP were shown to function as activators and inhibitors in Turing patterning [9]. Because the original Turing model assumes the initial condition is randomized, the resulting periodic patterns can vary stochastically. How does the regular hexagonal pattern happen? Experiments using reconstitution of a feather epithelium with dissociated mesenchymal cells help dissect the process, and suggest the propagation of the feather forming wave results from the combination of a local Turing patterning process with a global signaling event [6]. In the *in vitro* experiment, the whole skin explant is a morphogenetic field. *In vivo*, with constraints imposed by the global event, a narrow stripe of the propagating morphogenetic field is the only place that can support periodic patterning which later spreads bilaterally, thus giving the orderly appearance. However, the cellular and molecular basis of the global event and how the global event is coupled to the local Turing events were not identified previously.

Several more parameters must be considered when one thinks about the local interactions among skin progenitors. One being the intrinsic factors, which predetermines the responsive threshold of a cell, meaning cells must be in a competent state to respond to the activator and inhibitors in the environment. Molecularly this can

be translated as the number of morphogen receptors and the sensitivity threshold (e.g., FGF, BMP receptor, epigenetic states, etc.) or the amount of adhesion molecules expressed on the progenitor cell surface. The other is the extrinsic factors, including the amounts of morphogens (e.g., Wnt, FGF, BMP) or extracellular matrix molecules. These factors have to be within the right ratios and distribution to allow cells to launch Turing patterning.

Recently, the Turing concept has also been expanded beyond diffusible morphogens, and cell-cell adhesion or repulsion can mediate the activation or inhibitory function to reach Turing patterning without diffusion [10–12]. In the feather system, dynamic mesenchymal cell migration was observed [13] and local aggregation of mesenchymal cells and long-range tensile forces acting against tissue deformation may be caused by cell aggregation. Mesenchymal cell contraction may change β-catenin activity in epithelia and drive WNT signaling leading to the patterning [14]. It is the sum of these activators and inhibitors that drive the Turing patterning process within the morphogenetic field, whether they are in the form of diffusible morphogens or cell adhesive force, and whether they are generated by local or global events (Fig. 1A).

On top of this local Turing event, when a directed global event breaks the symmetry, it can trigger Turing patterning on an asymmetric field [15], manifested as a propagating patterning wave. In this issue, Ho et al. [1] analyzed the molecular network that generates the periodic feather array and provide new clues for us to understand the molecular circuit operating in the propagation of the morphogenetic wave.

FGF 20/ BMP4 feedback loop that facilitates Turing patterning locally

Ho et al. began by investigating the relationship between the FGF20/BMP4 pathway and mesenchymal cell aggregation in developing chick feathers. When beads soaked with FGF9 protein are placed on the competent skin field, mesenchymal cell aggregation and FGF20/BMP4 up-regulation were observed. Importantly, this up-regulation was inhibited if mesenchymal cell condensation was suppressed by an inhibitor for cell migration. This means cell aggregation plays a critical role in inducing downstream signals. Further, BMP signals inhibit FGF expression. Thus, FGF signaling forms a localized positive feedback loop through mesenchymal cell aggregation and the BMP signal works as a long-range inhibitor of FGF expression. This network has the basic characteristics required for Turing reaction-diffusion production of periodic patterning.

EDA wave as the global event

Based on the observed order of feather appearance in chicken embryos, the authors asked how the regular periodic pattern is formed. A computer simulation based on their findings suggests the existence of a traveling wave interacting with the Turing model factors could produce the highly ordered hexagonal feather array, and sequential feather formation from the midline to the lateral edge of the skin. When cell migration is suppressed transiently *ex vivo*, the order of feather array was distorted, suggesting the traveling wave is important in organizing molecular signaling and cell aggregation for feather patterning.

What is the cellular and molecular bases of this traveling wave? Recent studies imply that mechanical properties may play a role in feather array formation [13]. To evaluate whether mechanical force is the basis of the global wave, Ho et al. cut a piece of the skin explant and kept it away from the scaffold to allow the explant to contract in *in vitro* culture. Local tissue contraction did not change the position and the timing of feather formation, implying mechanical force is not the global wave and different factors are required to guide the propagation of the feather forming wave.

The mRNA expression of Ectodysplasin (EDA) suggests it may be a candidate [16]. It first emerges in the midline as a longitudinal stripe, then spreads bilaterally. EDA is a diffusible protein and is shown to induce FGF20 expression through binding of the EDA receptor (EDAR). In this process, beta-catenin (CTNNB1) was observed to be expressed globally in the dorsal skin, defining the morphogenetic field [6]. As the EDA wave progresses laterally, the global CTNNB1 expression regresses, and is replaced by enhanced CTNNB1 expression in each feather primordium that forms from the midline to the lateral edge. This moving wave front helps define the precise position of newly formed feather primordia.

When the EDA pathway is upregulated, width of FGF20 expression region is increased. Conversely, down-regulation of the EDA pathway decreased the width of the FGF 20 expression zone. Interestingly, in FGF20 chicken mutant skin, the EDA wave is still observed. Therefore, FGF20 signaling is not required for global wave propagation.

Cell density has been shown to set up the threshold of feather formation (Fig. 1B). Using the skin reconstitution experiments with different mesenchymal cell density, feather germs start to emerge when the cell density reaches a threshold to launch Turing patterning. But the hexagonal-like feather array is not reached until feather germs reach the highest packaging density [6]. They further investigated the interaction between EDA waves and mesenchymal cell density (Fig. 1C). Reducing cell density by inhibiting cell proliferation led to a narrower feather tract, yet the EDA expression wave was not

affected. Thus, mesenchymal cell density does not control the molecular wave. Yet, EDA seemingly affects the mesenchymal cell property that senses the environment. Interestingly, activation of EDA appears to allow mesenchymal cells to initiate periodic patterning at lower cell density. Thus, mesenchymal cells can sense their environment (cell density in this case) but their function (periodic patterning) is regulated by the chemical factor, EDA.

Cell adhesion and a mechano-chemical coupling loop

Mechanical force has now been shown to be one of the driving forces in development. Cell growth, as it increases cell density, generates mechanical stress in the environment surrounding the growing cell. These mechanical interactions are shown to be essential for the morphogenetic process [17]. Feather primordium formation is characterized by increased cell density and cell migration, which leads to dermal condensation. The increase in cell density can be achieved by cell proliferation or cell clustering. In cell clustering, cells migrate and adhere to form condensations. When Latrunculin A, an inhibitor of actin filament polymerization, abrogated cell migration by hampering force generation, it in turns disrupted primordium formation. In feathers, N-CAM serves as one of the adhesion molecules mediating dermal condensation formation [6]. Directional cell migration also plays a key driving force behind hair placode morphogenesis during mouse skin development [18]. Externally applied force via cell constraint, activates Pax9 in a mesenchymal condensation during embryonic tooth germ formation [19]. Together these findings show that mechanical force, achieved through high cell density, cell migration and / or adhesion, could serve as an activator that turns on key signals required to engage cell collectives in Turing patterning. We can also state that mechanical force contributes to the side of Turing activator, and it is the sum of Turing activator and inhibitors that cells use to make decisions on whether to enter Turing patterning (Fig. 1A). Thus, this is a chemo-mechanical coupling event that should be fundamentally observed in many other model systems.

Irregular feather patterns on the skin of flightless birds: emus and ostriches

Ho et al. then compare the distribution of feather buds on the trunk of flightless birds. Feather buds on ostrich and emu embryos tend to show less ordered feather arrays as compared with those in flying birds. Further analyses showed ostrich embryos display no EDA wave, which seems to be the reason for less ordered feather patterns. In emus, the mechanism appears to be different. Emu skin loses EDA wave's guidance of patterning, but it still effectively shows defined feather tracts. We hence reason that a

defect on the mesenchymal cell during early pattern formation may play a greater role here. In emus, the densification of mesenchymal cells is extremely delayed, missing the timing to interact with molecular factors. Thus, ostriches and emus may have independently acquired different ways to keep their irregular feather arrays. This irregular periodic patterning may be due to the lower demand to acquire regularly arranged contour feathers required for flight. Thus, Turing patterning can form in combination or not in combination with a global traveling wave to have different feather array patterns (Fig. 2).

Outlook

The periodic feather arrays are formed by local cell-cell interactions that satisfy the requirements needed for Turing patterning. This system can define the periodicity of the pattern but cannot set the specific feather array pattern. Global mechanisms such as traveling waves that traverse the whole skin generate the timing and positioning of patterning within a morphogenetic field.

Biological waves act at many levels in living systems: Calcium ion waves after frog egg fertilization, actin assembly waves in cell migration, cAMP waves leading to slime mold pattern formation, etc. Given that our body is composed of highly-ordered tissues, a combination of local and global control may be a fundamental process to reinforce the accuracy and robustness of morphogenesis.

This work has nicely presented the molecular components of the global wave in feather array formation, and how the global wave is coupled to the local Turing patterning process. They also elegantly use emu and ostrich skin to contrast the different patterning mechanisms. Yet there are also many unsolved questions. For example, the authors did not explore how the EDA wave propagates. How EDA modulates the threshold of mesenchymal cells in the context of mechano-chemical coupling will need to be elaborated in future studies. How do mesenchymal cells sense the environment? When will the EDA wave stop and how the tract boundaries are set are also interesting unsolved questions. This paper is a good step toward understanding these wonderful biological examples of periodic pattern formation.

Figure legends

Fig 1. Turing model and its molecular cellular mechanisms.
(A) Hypothetical molecular network generating Turing patterns. In the short range, an activator (A) enhances its own production and that of an inhibitor (I). In the long range, the inhibitor suppresses the production of the activator. Right figures are examples of resulting Turing patterns. Molecular factors and cellular interactions involved in the Turing model are summarized in the table. (B) Reconstitution of skin explants exhibit feather bud (red circles) formation depending on the mesenchymal cell density. There is a cell density threshold required to initiate bud formation and a cell density threshold required to reach maximum bud density (red line). (C) A travelling EDA wave (blue) moving in the medial-lateral direction (x axis) at each time point (T1-3). EDA signaling adds to activator, decreases the threshold (red line) of required mesenchymal cell density (y axis) to initiate feather bud formation. Red broken circles and red circles present feather buds during and after patterning, respectively.

Fig 2. Feather array formation with and without a global wave.
(A) In the reconstituting skin explant, the morphogenetic field (blue) are static, leading to the simultaneous formation of a less-ordered feather (red circle) array. (B) In flightless birds, this less-ordered feather array is formed due to the static morphogenetic field. (C) In *in vivo* flight birds, the high-ordered feather array is formed sequentially from the midline to lateral regions by the morphogenetic waves that travel bilaterally.

References

1. Ho et al. Feather Arrays are Patterned by Interacting Signalling and Cell Density Waves
2. Sengel P (1990) Pattern formation in skin development. Int J Dev Biol 34: 33–50.
3. Michon F, Forest L, Collomb E, Demongeot J, Dhouailly D (2008) BMP2 and BMP7 play antagonistic roles in feather induction. Development 135: 2797–2805. doi:10.1242/dev.018341.
4. Jiang T-X, Widelitz RB, Shen W-M, Will P, Wu D-Y, et al. (2004) Integument pattern formation involves genetic and epigenetic controls: feather arrays simulated by digital hormone models. Int J Dev Biol 48: 117–135. doi:10.1387/ijdb.041788tj.
5. Davidson D (1983) The mechanism of feather pattern development in the chick. 1. The time of determination of feather position. J Embryol Exp Morphol 74: 245–259.
6. Jiang TX, Jung HS, Widelitz RB, Chuong CM (1999) Self-organization of periodic patterns by dissociated feather mesenchymal cells and the regulation of size, number and spacing of primordia. Development 126: 4997–5009.
7. Turing AM (1952) The Chemical Basis of Morphogenesis. Philos Trans R Soc Lond B, Biol Sci 237: 37–72. doi:10.1098/rstb.1952.0012.
8. Meinhardt H (1982) Models of biological pattern formation. London: Academic Press.
9. Jung HS, Francis-West PH, Widelitz RB, Jiang TX, Ting-Berreth S, et al. (1998) Local inhibitory action of BMPs and their relationships with activators in feather formation: implications for periodic patterning. Dev Biol 196: 11–23. doi:10.1006/dbio.1998.8850.
10. Inaba M, Yamanaka H, Kondo S (2012) Pigment pattern formation by contact-dependent depolarization. Science 335: 677. doi:10.1126/science.1212821.
11. Hamada H, Watanabe M, Lau HE, Nishida T, Hasegawa T, et al. (2014) Involvement of Delta/Notch signaling in zebrafish adult pigment stripe patterning. Development 141: 318–324. doi:10.1242/dev.099804.
12. Kondo S (2017) An updated kernel-based Turing model for studying the mechanisms of biological pattern formation. J Theor Biol 414: 120–127. doi:10.1016/j.jtbi.2016.11.003.

13. Lin C-M, Jiang TX, Baker RE, Maini PK, Widelitz RB, et al. (2009) Spots and stripes: pleomorphic patterning of stem cells via p-ERK-dependent cell chemotaxis shown by feather morphogenesis and mathematical simulation. Dev Biol 334: 369–382. doi:10.1016/j.ydbio.2009.07.036.
14. Shyer AE, Rodrigues AR, Schroeder GG, Kassianidou E, Kumar S, et al. (2017) Emergent cellular self-organization and mechanosensation initiate follicle pattern in the avian skin. Science 357: 811–815. doi:10.1126/science.aai7868.
15. Cruywagen GC, Maini PK, Murray JD (1992) Sequential pattern formation in a model for skin morphogenesis. IMA J Math Appl Med Biol 9: 227–248.
16. Drew CF, Lin CM, Jiang TX, Blunt G, Mou C, et al. (2007) The Edar subfamily in feather placode formation. Dev Biol 305: 232–245. doi:10.1016/j.ydbio.2007.02.011.
17. LeGoff L, Lecuit T (2015) Mechanical forces and growth in animal tissues. Cold Spring Harb Perspect Biol 8: a019232. doi:10.1101/cshperspect.a019232.
18. Ahtiainen L, Lefebvre S, Lindfors PH, Renvoisé E, Shirokova V, et al. (2014) Directional cell migration, but not proliferation, drives hair placode morphogenesis. Dev Cell 28: 588–602. doi:10.1016/j.devcel.2014.02.003.
19. Mammoto T, Mammoto A, Torisawa Y, Tat T, Gibbs A, et al. (2011) Mechanochemical control of mesenchymal condensation and embryonic tooth organ formation. Dev Cell 21: 758–769. doi:10.1016/j.devcel.2011.07.006.

Turing patterning with and without a global wave

Masafumi Inaba[1], Hans I-Chen Harn[1,2], and Cheng-Ming Chuong[1,2,3]

Author Affiliations:

[1] Department of Pathology, Keck School of Medicine, University of Southern California, Los Angeles, CA, USA

[2] International Research Center of Wound Repair and Regeneration (iWRR), National Cheng Kung University, Tainan, Taiwan

[3] Integrative Stem Cell Center, China Medical University Hospital, China Medical University, Taichung, Taiwan

Funding:

M.I. is supported by Human Frontier Science Program (LT001148/2015-L). HIH is supported by grant from Ministry of Education of Taiwan. CMC is supported by NIH Grants AR47364, AR60306, and GM125322.

Abstract

Periodic patterning represents a fundamental process in tissue morphogenesis. In chicken dorsal skin, feather formation starts from the midline, then the morphogenetic wave propagates bilaterally, leaving a regular hexagonal array of feather germs. Yet, in vitro reconstitution showed feather germs appear simultaneously, leading to the hypothesis that the feather-forming wave results from the coupling of local Turing patterning processes with an unidentified global event. In this issue, Ho et al. (1), showed such a global event in chicken feathers involves a spreading EDA wave and FGF20-cell aggregate-based mechano-chemical coupling. Interestingly, in flightless birds, feather germs form without waves are irregularly positioned.

Regular periodic feather patterns on the chicken skin

Animal integuments exhibit periodic patterns in spots, stripes or mazes, which are made of pigment domains, hairs or feathers. In the developing chicken embryo, one of the most fascinating phenomena is that feather buds begin to form at the dorsal midline around embryonic day 6, then propagate bilaterally toward the flank, leaving a highly ordered array of feather germs arranged in a hexagonal pattern after about three days [2–4].

Is this patterning process a playout of a molecular blueprint (like in Drosophila) or the result of stochastic local interactions? Perturbation experiments leading to altered patterns suggest the system is plastic [5,6] and skin progenitors are not pre-determined to be a bud or an interbud cell. For local interactions, one fundamental theory is based on Turing's reaction-diffusion) model [7,8]. Turing showed hypothetical chemical reactions could form periodic structures spontaneously in a situation where an activator activates its own production and a long-range inhibitor that represses the activator. When the inhibitor diffusion rate is much larger than that of activator, those chemicals are distributed heterogeneously, forming periodic patterns such as spots and stripes.

In feathers, FGF and BMP were shown to function as activators and inhibitors in Turing patterning [9]. Because the original Turing model assumes the initial condition is randomized, the resulting periodic patterns can vary stochastically. How does the regular hexagonal pattern happen? Experiments using reconstitution of a feather epithelium with dissociated mesenchymal cells help dissect the process, and suggest the propagation of the feather forming wave results from the combination of a local Turing patterning process with a global signaling event [6]. In the *in vitro* experiment, the whole skin explant is a morphogenetic field. *In vivo*, with constraints imposed by the global event, a narrow stripe of the propagating morphogenetic field is the only place that can support periodic patterning which later spreads bilaterally, thus giving the orderly appearance. However, the cellular and molecular basis of the global event and how the global event is coupled to the local Turing events were not identified previously.

Several more parameters must be considered when one thinks about the local interactions among skin progenitors. One being the intrinsic factors, which predetermines the responsive threshold of a cell, meaning cells must be in a competent state to respond to the activator and inhibitors in the environment. Molecularly this can be translated as the number of morphogen receptors and the sensitivity threshold (e.g.,

FGF, BMP receptor, epigenetic states, etc.) or the amount of adhesion molecules expressed on the progenitor cell surface. The other is the extrinsic factors, including the amounts of morphogens (e.g., Wnt, FGF, BMP) or extracellular matrix molecules. These factors have to be within the right ratios and distribution to allow cells to launch Turing patterning.

Recently, the Turing concept has also been expanded beyond diffusible morphogens, and cell-cell adhesion or repulsion can mediate the activation or inhibitory function to reach Turing patterning without diffusion [10–12]. In the feather system, dynamic mesenchymal cell migration was observed [13] and local aggregation of mesenchymal cells and long-range tensile forces acting against tissue deformation may be caused by cell aggregation. Mesenchymal cell contraction may change β-catenin activity in epithelia and drive WNT signaling leading to the patterning [14]. It is the sum of these activators and inhibitors that drive the Turing patterning process within the morphogenetic field, whether they are in the form of diffusible morphogens or cell adhesive force, and whether they are generated by local or global events (Fig. 1A).

On top of this local Turing event, when a directed global event breaks the symmetry, it can trigger Turing patterning on an asymmetric field [15], manifested as a propagating patterning wave. In this issue, Ho et al. [1] analyzed the molecular network that generates the periodic feather array and provide new clues for us to understand the molecular circuit operating in the propagation of the morphogenetic wave.

FGF 20/ BMP4 feedback loop that facilitates Turing patterning locally

Ho et al. began by investigating the relationship between the FGF20/BMP4 pathway and mesenchymal cell aggregation in developing chick feathers. When beads soaked with FGF9 protein are placed on the competent skin field, mesenchymal cell aggregation and FGF20/BMP4 up-regulation were observed. Importantly, this up-regulation was inhibited if mesenchymal cell condensation was suppressed by an inhibitor for cell migration. This means cell aggregation plays a critical role in inducing downstream signals. Further, BMP signals inhibit FGF expression. Thus, FGF signaling forms a localized positive feedback loop through mesenchymal cell aggregation and the BMP signal works as a long-range inhibitor of FGF expression. This network has the basic characteristics required for Turing reaction-diffusion production of periodic patterning.

EDA wave as the global event

Based on the observed order of feather appearance in chicken embryos, the authors asked how the regular periodic pattern is formed. A computer simulation based on their findings suggests the existence of a traveling wave interacting with the Turing model factors could produce the highly ordered hexagonal feather array, and sequential feather formation from the midline to the lateral edge of the skin. When cell migration is suppressed transiently *ex vivo*, the order of feather array was distorted, suggesting the traveling wave is important in organizing molecular signaling and cell aggregation for feather patterning.

What is the cellular and molecular bases of this traveling wave? Recent studies imply that mechanical properties may play a role in feather array formation [13]. To evaluate whether mechanical force is the basis of the global wave, Ho et al. cut a piece of the skin explant and kept it away from the scaffold to allow the explant to contract in *in vitro* culture. Local tissue contraction did not change the position and the timing of feather formation, implying mechanical force is not the global wave and different factors are required to guide the propagation of the feather forming wave.

The mRNA expression of Ectodysplasin (EDA) suggests it may be a candidate [16]. It first emerges in the midline as a longitudinal stripe, then spreads bilaterally. EDA is a diffusible protein and is shown to induce FGF20 expression through binding of the EDA receptor (EDAR). In this process, beta-catenin (CTNNB1) was observed to be expressed globally in the dorsal skin, defining the morphogenetic field [6]. As the EDA wave progresses laterally, the global CTNNB1 expression regresses, and is replaced by enhanced CTNNB1 expression in each feather primordium that forms from the midline to the lateral edge. This moving wave front helps define the precise position of newly formed feather primordia.

When the EDA pathway is upregulated, width of FGF20 expression region is increased. Conversely, down-regulation of the EDA pathway decreased the width of the FGF 20 expression zone. Interestingly, in FGF20 chicken mutant skin, the EDA wave is still observed. Therefore, FGF20 signaling is not required for global wave propagation.

Cell density has been shown to set up the threshold of feather formation. Using the skin reconstitution experiments with different mesenchymal cell density, feather germs start to emerge when the cell density reaches a threshold to launch Turing patterning. But the hexagonal-like feather array is not reached until feather germs reach the highest packaging density [6]. They further investigated the interaction between EDA waves and mesenchymal cell density (Fig. 1C). Reducing cell density by inhibiting cell proliferation led to a narrower feather tract, yet the EDA expression wave was not affected. Thus, mesenchymal cell density does not control the molecular wave. Yet, EDA

seemingly affects the mesenchymal cell property that senses the environment. Interestingly, activation of EDA appears to allow mesenchymal cells to initiate periodic patterning at lower cell density. Thus, mesenchymal cells can sense their environment (cell density in this case) but their function (periodic patterning) is regulated by the chemical factor, EDA.

Cell adhesion and a mechano-chemical coupling loop

Mechanical force has now been shown to be one of the driving forces in development. Cell growth, as it increases cell density, generates mechanical stress in the environment surrounding the growing cell. These mechanical interactions are shown to be essential for the morphogenetic process [17]. Feather primordium formation is characterized by increased cell density and cell migration, which leads to dermal condensation. The increase in cell density can be achieved by cell proliferation or cell clustering. In cell clustering, cells migrate and adhere to form condensations. When Latrunculin A, an inhibitor of actin filament polymerization, abrogated cell migration by hampering force generation, it in turns disrupted primordium formation. In feathers, N-CAM serves as one of the adhesion molecules mediating dermal condensation formation [6]. Directional cell migration also plays a key driving force behind hair placode morphogenesis during mouse skin development [18]. Externally applied force via cell constraint, activates Pax9 in a mesenchymal condensation during embryonic tooth germ formation [19]. Together these findings show that mechanical force, achieved through high cell density, cell migration and / or adhesion, could serve as an activator that turns on key signals required to engage cell collectives in Turing patterning. We can also state that mechanical force contributes to the side of Turing activator, and it is the sum of Turing activator and inhibitors that cells use to make decisions on whether to enter Turing patterning (Fig. 1A). Thus, this is a chemo-mechanical coupling event that should be fundamentally observed in many other model systems.

Irregular feather patterns on the skin of flightless birds: emus and ostriches

Ho et al. then compare the distribution of feather buds on the trunk of flightless birds. Feather buds on ostrich and emu embryos tend to show less ordered feather arrays as compared with those in flying birds. Further analyses showed ostrich embryos display no EDA wave, which seems to be the reason for less ordered feather patterns. In emus, the mechanism appears to be different. Emu skin loses EDA wave's guidance of patterning, but it still effectively shows defined feather tracts. We hence reason that a defect on the mesenchymal cell during early pattern formation may play a greater role

here. In emus, the densification of mesenchymal cells is extremely delayed, missing the timing to interact with molecular factors. Thus, ostriches and emus may have independently acquired different ways to keep their irregular feather arrays. This irregular periodic patterning may be due to the lower demand to acquire regularly arranged contour feathers required for flight. Thus, Turing patterning can form in combination or not in combination with a global traveling wave to have different feather array patterns (Fig. 2).

Outlook

The periodic feather arrays are formed by local cell-cell interactions that satisfy the requirements needed for Turing patterning. This system can define the periodicity of the pattern but cannot set the specific feather array pattern. Global mechanisms such as traveling waves that traverse the whole skin generate the timing and positioning of patterning within a morphogenetic field.

Biological waves act at many levels in living systems: Calcium ion waves after frog egg fertilization, actin assembly waves in cell migration, cAMP waves leading to slime mold pattern formation, etc. Given that our body is composed of highly-ordered tissues, a combination of local and global control may be a fundamental process to reinforce the accuracy and robustness of morphogenesis.

This work has nicely presented the molecular components of the global wave in feather array formation, and how the global wave is coupled to the local Turing patterning process. They also elegantly use emu and ostrich skin to contrast the different patterning mechanisms. Yet there are also many unsolved questions. For example, the authors did not explore how the EDA wave propagates. How EDA modulates the threshold of mesenchymal cells in the context of mechano-chemical coupling will need to be elaborated in future studies. How do mesenchymal cells sense the environment? When will the EDA wave stop and how the tract boundaries are set are also interesting unsolved questions. This paper is a good step toward understanding these wonderful biological examples of periodic pattern formation.

Figure legends

Fig 1. Turing model and its molecular cellular mechanisms.
(A) Hypothetical molecular network generating Turing patterns. In the short range, an activator (A) enhances its own production and that of an inhibitor (I). In the long range, the inhibitor suppresses the production of the activator. Right figures are examples of resulting Turing patterns. Molecular factors and cellular interactions involved in the Turing model are summarized in the table. (B) Reconstitution of skin explants exhibit feather bud (red circles) formation depending on the mesenchymal cell density. There is a cell density threshold required to initiate bud formation and a cell density threshold required to reach maximum bud density (red line). (C) A travelling EDA wave (blue) moving in the medial-lateral direction (x axis) at each time point (T1-3). EDA signaling adds to activator, decreases the threshold (red line) of required mesenchymal cell density (y axis) to initiate feather bud formation. Red broken circles and red circles present feather buds during and after patterning, respectively.

Fig 2. Feather array formation with and without a global wave.
(A) In the reconstituting skin explant, the morphogenetic field (blue) are static, leading to the simultaneous formation of a less-ordered feather (red circle) array. (B) In flightless birds, this less-ordered feather array is formed due to the static morphogenetic field. (C) In *in vivo* flight birds, the high-ordered feather array is formed sequentially from the midline to lateral regions by the morphogenetic waves that travel bilaterally.

References

1. Ho et al. Feather Arrays are Patterned by Interacting Signalling and Cell Density Waves
2. Sengel P (1990) Pattern formation in skin development. Int J Dev Biol 34: 33–50.
3. Michon F, Forest L, Collomb E, Demongeot J, Dhouailly D (2008) BMP2 and BMP7 play antagonistic roles in feather induction. Development 135: 2797–2805. doi:10.1242/dev.018341.
4. Jiang T-X, Widelitz RB, Shen W-M, Will P, Wu D-Y, et al. (2004) Integument pattern formation involves genetic and epigenetic controls: feather arrays simulated by digital hormone models. Int J Dev Biol 48: 117–135. doi:10.1387/ijdb.041788tj.
5. Davidson D (1983) The mechanism of feather pattern development in the chick. 1. The time of determination of feather position. J Embryol Exp Morphol 74: 245–259.
6. Jiang TX, Jung HS, Widelitz RB, Chuong CM (1999) Self-organization of periodic patterns by dissociated feather mesenchymal cells and the regulation of size, number and spacing of primordia. Development 126: 4997–5009.
7. Turing AM (1952) The Chemical Basis of Morphogenesis. Philos Trans R Soc Lond B, Biol Sci 237: 37–72. doi:10.1098/rstb.1952.0012.
8. Meinhardt H (1982) Models of biological pattern formation. London: Academic Press.
9. Jung HS, Francis-West PH, Widelitz RB, Jiang TX, Ting-Berreth S, et al. (1998) Local inhibitory action of BMPs and their relationships with activators in feather formation: implications for periodic patterning. Dev Biol 196: 11–23. doi:10.1006/dbio.1998.8850.
10. Inaba M, Yamanaka H, Kondo S (2012) Pigment pattern formation by contact-dependent depolarization. Science 335: 677. doi:10.1126/science.1212821.
11. Hamada H, Watanabe M, Lau HE, Nishida T, Hasegawa T, et al. (2014) Involvement of Delta/Notch signaling in zebrafish adult pigment stripe patterning. Development 141: 318–324. doi:10.1242/dev.099804.
12. Kondo S (2017) An updated kernel-based Turing model for studying the mechanisms of biological pattern formation. J Theor Biol 414: 120–127. doi:10.1016/j.jtbi.2016.11.003.

13. Lin C-M, Jiang TX, Baker RE, Maini PK, Widelitz RB, et al. (2009) Spots and stripes: pleomorphic patterning of stem cells via p-ERK-dependent cell chemotaxis shown by feather morphogenesis and mathematical simulation. Dev Biol 334: 369–382. doi:10.1016/j.ydbio.2009.07.036.
14. Shyer AE, Rodrigues AR, Schroeder GG, Kassianidou E, Kumar S, et al. (2017) Emergent cellular self-organization and mechanosensation initiate follicle pattern in the avian skin. Science 357: 811–815. doi:10.1126/science.aai7868.
15. Cruywagen GC, Maini PK, Murray JD (1992) Sequential pattern formation in a model for skin morphogenesis. IMA J Math Appl Med Biol 9: 227–248.
16. Drew CF, Lin CM, Jiang TX, Blunt G, Mou C, et al. (2007) The Edar subfamily in feather placode formation. Dev Biol 305: 232–245. doi:10.1016/j.ydbio.2007.02.011.
17. LeGoff L, Lecuit T (2015) Mechanical forces and growth in animal tissues. Cold Spring Harb Perspect Biol 8: a019232. doi:10.1101/cshperspect.a019232.
18. Ahtiainen L, Lefebvre S, Lindfors PH, Renvoisé E, Shirokova V, et al. (2014) Directional cell migration, but not proliferation, drives hair placode morphogenesis. Dev Cell 28: 588–602. doi:10.1016/j.devcel.2014.02.003.
19. Mammoto T, Mammoto A, Torisawa Y, Tat T, Gibbs A, et al. (2011) Mechanochemical control of mesenchymal condensation and embryonic tooth organ formation. Dev Cell 21: 758–769. doi:10.1016/j.devcel.2011.07.006.

A

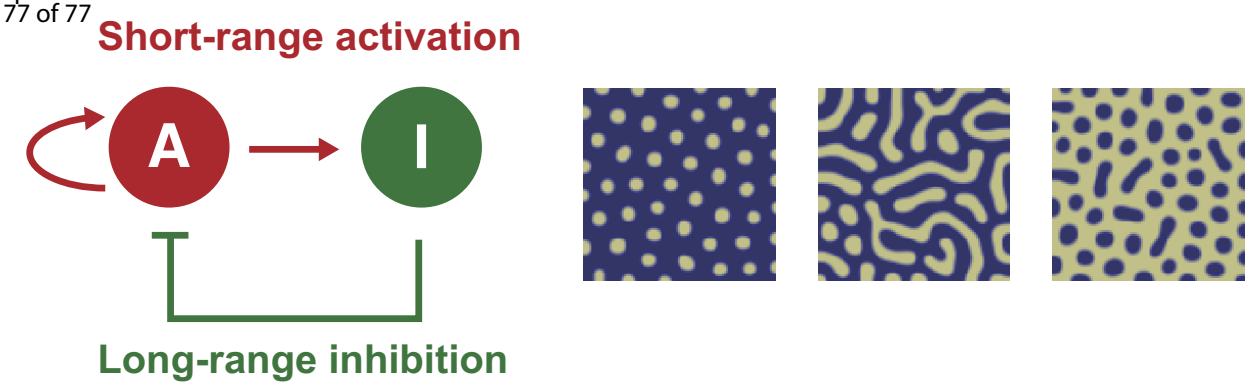

	Short range	Long range
Morphogens	Fgf, Wnt, Nodal	Dkk, Bmp, Lefty
Cell interactions	Cell repulsion	Long fillopodia
Mechano-chemo coupling	Cell condensation	Tensile force

B

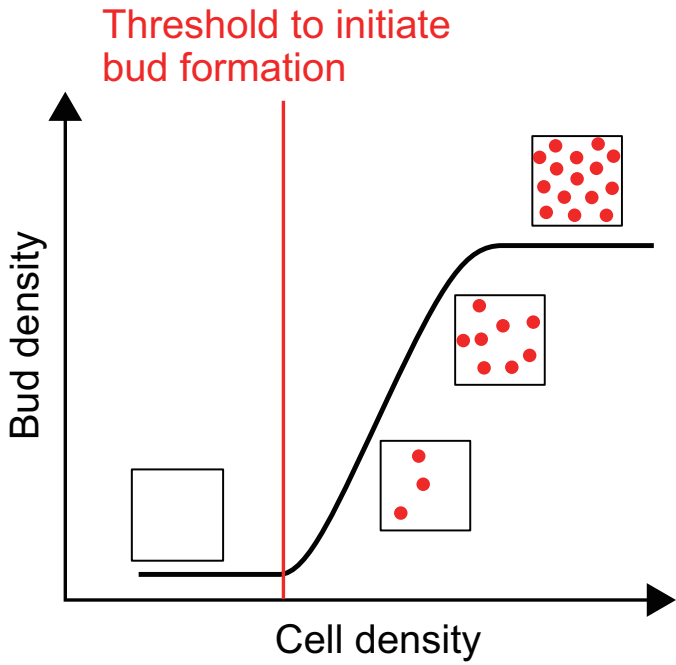

C